

Project acronym:	GeoHex		
Project title:	Advanced material for cost-efficient and enhanced heat exchange performance for geothermal application		
Activity:	LC-CS3-RES-1-2019-2020 Developing the next generation of renewable energy technologies		
Call:	H2020-LC-CS3-2019-RES-TwoStages		
Funding Scheme:	RIA	Grant Agreement No:	851917
WP1	Requirement analysis and project mapping		

D1.1 – Analysis of HX technologies for geothermal & HXs structures

Due date:	29/02/2020 (M4)	
Actual Submission Date:	31/03/2020	
Lead Beneficiary:	CEA	
Main authors/contributors:	Z. Minvielle (CEA), F. Pra (CEA)	
Dissemination Level¹:	PU	
Nature:	Report	
Status of this version:		Draft under Development
		For Review by Coordinator
	X	Submitted
Version:	V1	
Abstract	The deliverable reports on the structure of heat exchangers that will be used to demonstrate materials improvements.	

REVISION HISTORY

Version	Date	Main Authors/Contributors	Description of changes
V1	20/02/2020	CEA – Z. Minvielle, F. Pra	
V2	24/03/2020	CEA – Z. Minvielle, F. Pra	Addition of the benchmark study



This project has received funding from the European Union's Horizon 2020 Research and Innovation programme under grant agreement No. 851917

¹ Dissemination level security:

PU – Public (e.g. on website, for publication etc.) / **PP** – Restricted to other programme participants (incl. Commission services) /

RE – Restricted to a group specified by the consortium (incl. Commission services) / **CO** – confidential, only for members of the consortium (incl. Commission services)



This project has received funding from the European Union's Horizon 2020 program Grant Agreement No 851917. This publication reflects the views only of the author(s), and the Commission cannot be held responsible for any use which may be made of the information contained therein.

Copyright © 2019-2022, GeoHex Consortium

This document and its contents remain the property of the beneficiaries of the GeoHex Consortium and may not be distributed or reproduced without the express written approval of the Geo-Drill Coordinator, TWI Ltd. (www.twi-global.com)

THIS DOCUMENT IS PROVIDED BY THE COPYRIGHT HOLDERS AND CONTRIBUTORS "AS IS" AND ANY EXPRESS OR IMPLIED WARRANTIES, INCLUDING, BUT NOT LIMITED TO, THE IMPLIED WARRANTIES OF MERCHANTABILITY AND FITNESS FOR A PARTICULAR PURPOSE ARE DISCLAIMED. IN NO EVENT SHALL THE COPYRIGHT OWNER OR CONTRIBUTORS BE LIABLE FOR ANY DIRECT, INDIRECT, INCIDENTAL, SPECIAL, EXEMPLARY, OR CONSEQUENTIAL DAMAGES (INCLUDING, BUT NOT LIMITED TO, PROCUREMENT OF SUBSTITUTE GOODS OR SERVICES; LOSS OF USE, DATA, OR PROFITS; OR BUSINESS INTERRUPTION) HOWEVER CAUSED AND ON ANY THEORY OF LIABILITY, WHETHER IN CONTRACT, STRICT LIABILITY, OR TORT (INCLUDING NEGLIGENCE OR OTHERWISE) ARISING IN ANY WAY OUT OF THE USE OF THIS DOCUMENT, EVEN IF ADVISED OF THE POSSIBILITY OF SUCH DAMAGE.

CONTENTS

1.	EXECUTIVE SUMMARY	4
2.	OBJECTIVES MET	4
3.	INTRODUCTION	4
4.	SOA METHODOLOGY.....	4
4.1	OVERVIEW	4
4.2	GEOTHERMAL POWER PLANTS.....	5
4.2.1	General considerations	5
4.2.2	Electricity production cycles	5
4.2.3	Patents analysis.....	9
4.3	ORGANIC RANKINE CYCLE	11
4.3.1	Working fluids	11
4.3.2	Operating data – Case studies	17
4.3.3	Heat exchangers.....	31
4.3.3.1	Overview	31
4.3.3.2	Evaporators.....	31
4.3.3.3	Recuperators/preheaters.....	36
4.3.3.4	Condensers.....	37
4.3.3.5	Heat exchanger modelling	41
4.3.3.6	Patents analysis.....	42
5.	CONCLUSIONS	45
6.	REFERENCES	47

1. EXECUTIVE SUMMARY

This deliverable reports the state-of-the-art (SoA) of heat exchanger (HX) technologies relevant for geothermal applications. Following the general presentation of geothermal power plants involving organic Rankine cycle (ORC) systems and the list of worldwide binary-cycle plants, this report focuses on the HX main technologies and the operating conditions (working fluids, temperature, pressure, heat transfer coefficient, etc) of ORC systems. It concerns the evaporator, the condensers (water-cooled or air-cooled) and the one-phase HXs (pre-heater, recuperator). A patent analysis is also provided. The conclusion provides some considerations regarding the structure and the materials of the HXs that will be used to demonstrate material deposit improvements.

2. OBJECTIVES MET

This deliverable helps to meet the following work package objective:

- To identify the different and most relevant types of Heat Exchangers compatible with the geometry to be selected in the project.

3. INTRODUCTION

Heat exchangers (HXs) are the most critical components of a geothermal power plant, especially for organic Rankine cycle (ORC) based plant, and the capital cost of heat exchangers accounts for a large proportion of ORC. Because of corrosion and scaling due to geothermal brine, expensive HX materials are recommended, and degraded performance over time requires specification of excess capacity in the HXs. Hence, improvements in the antiscaling and anticorrosion properties as well as heat transfer performance of the HX material will lead to smaller, more efficient and less costly systems. To this end, the GeoHex project proposes to modify the HX surfaces with appropriate material deposits.

Prior to the scalability and manufacturability studies of the material deposits in commercial HX structures (WP5) and prior to the HX design and characterisation in an ORC experimental test rig (WP7), the HX technologies usually involved in geothermal power plants based on ORC system have to be reviewed. This is one of the objectives of WP1. In addition to deliverable D1.2, which focuses on the SoA materials for geothermal HXs, this deliverable reports the SoA of HX technologies relevant for geothermal applications. Following the general presentation of geothermal power plants involving ORC systems and the list of worldwide binary-cycle plants, this report focuses on the HX main technologies and the operating conditions (working fluids, temperature, pressure, heat transfer coefficient, etc) of ORC systems. It concerns the evaporator, the condensers (water-cooled or air-cooled) and the one-phase HXs (pre-heater, recuperator). The conclusion provides some considerations regarding the structure and the materials of the HXs that will be used to demonstrate material deposit improvements.

4. SOA METHODOLOGY

4.1 Overview

To provide relevant SoA of HX technologies, a bibliometric study questioning different databases has been performed. It includes scientific literature (research articles and scientific reviews), patents related to geothermal power plants and ORC manufacturers and public data analysis (web data and public reports).

4.2 Geothermal power plants

4.2.1 General considerations

In 2011, Tchanche et al. reported 504 geothermal power plants in operation in 27 countries with a total installed capacity of about 10 GW. Figure 1 illustrates the worldwide geographic distribution of binary-type geothermal power plants.

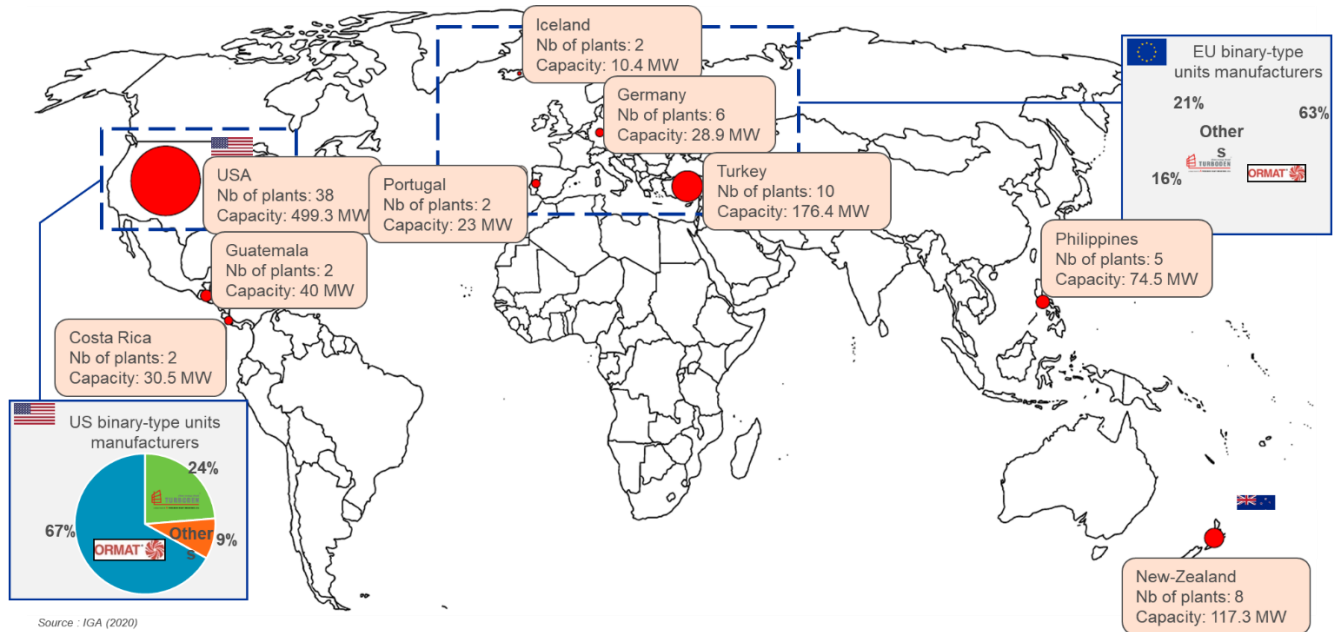


Figure 1: Geographic distribution of binary-type geothermal power plants.

In 2017 (Tomarov and Shipkov, 2017), the total installed capacity of geothermal binary power units in 25 countries increased by more than 50% over the past 5 years, reaching nearly 1800 MW (hereinafter electric power is indicated), by 2015. A vast majority of the existing binary power plants recovers heat of geothermal fluid in the range of 100–200°C. Binary cycle power plants have an average unit capacity of 6.3 MW, 30.4 MW at single-flash power plants, 37.4 MW at double-flash plants, and 45.4 MW at power plants working on superheated steam. The largest binary cycle geothermal power plants (GeoPP) with an installed capacity of over 60 MW are in operation in the United States and the Philippines.

4.2.2 Electricity production cycles

Major types of geothermal power plants are: dry steam, single-flash, double-flash and binary-cycle plants. A comparison between available options, from Tchanche et al. (2011), is summarised in Table 1. Flash systems are used for moderate and liquid-dominated resources, dry steam plants for dry-steam resources and binary cycles are well adapted for low-temperature liquid-dominated resources.

Table 1. Comparison of different types of geothermal plants.

Type	Resource temperature (°C)	Utilisation efficiency (%)	Plant cost and complexity
Double-flash	240–320	35–45	Moderate ► high
Dry-steam	180–300	50–65	Low-moderate
Single-flash	200–260	30–35	Moderate
Basic binary	125–165	25–45	Moderate ► high

The typical temperature range and power output according to the type of geothermal power plant is illustrated in Figure 2 (Guzovic et al., 2012):

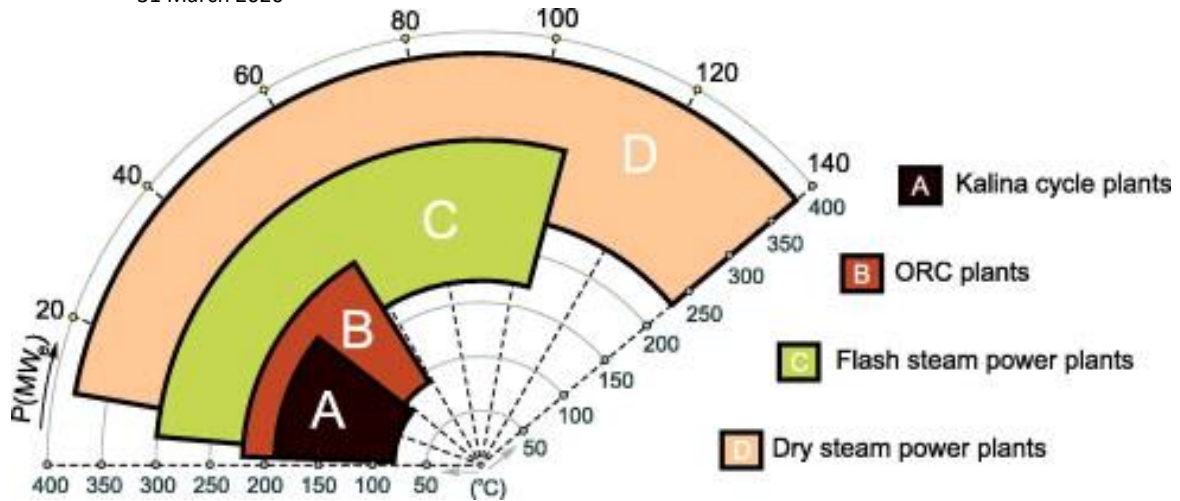


Figure 2. Application ranges of various types of geothermal power plants.

Binary cycle geothermal power generation plants differ from dry steam and flash steam systems in that the water or the steam from the geothermal reservoir never comes into contact with the turbine/generator units. In binary systems, the water from the geothermal reservoir is used to heat a secondary fluid, which is vaporised and used to turn the turbine/generator units. The geothermal water and the working fluid are each confined in separate circulating systems and never come into contact with each other.

Since the available temperature difference is less, the cycle efficiency (approximately 5–9%) is much lower than that of thermal power generation using medium temperature geothermal resources (approximately 10–15%). Further, in low-temperature systems, large heat exchanger areas are required to extract the same amount of energy compared with medium-temperature systems. These factors impose limits on exploiting low-temperature geothermal resources and emphasise the necessity of optimum, cost-effective design of binary power cycles (Hettiarachchi et al., 2007).

In a geothermal binary plant, the thermal energy of the geothermal fluid is transferred to a secondary working fluid via heat exchangers for use in a conventional Rankine cycle. Figure 3 is a schematic layout of an ORC system (Altun and Kilic, 2020).

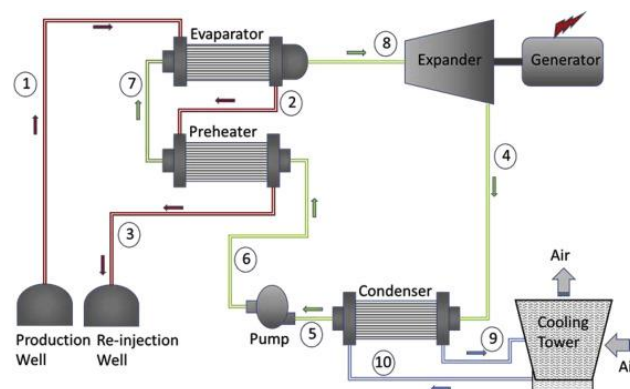


Figure 3. The schematic diagram of AFJET ORC power plant (Altun and Kilic, 2020).

The organic working fluid receives heat, evaporates and expands in the turbine before being condensed and returned back to the evaporator by the feed pump. Cooling of the condenser is assured by air coolers, surface water cooling systems, wet-type cooling towers or dry-type cooling towers. One of the first binary geothermal plant was put into operation at Paratunka, Russia in 1967. It was rated at 680 kW using water at a temperature of 81°C and this plant proved the feasibility of the binary concept. For low-temperature geothermal fluids below 150°C, it is difficult to implement cost effective flash steam plants and the binary option is the sole solution.

Date: 31 March 2020

DiPippo (2016) reported that in 2014 binary power plants were the most widely used type of geothermal power plant with 203 units, generating 1245 MW of power. They constituted over 35% of all geothermal units in operation but generated only 10% of the total power. The technology has been developed and commercialised since the 1980s by Ormat Technology Inc. In the MW power range; ORC modules incorporate conventional turbines and are cost-effective, while at lower power outputs the lack of cheap turbines renders the technology hardly applicable. *Brasz et al. (2005)* suggested using HVAC (heating, ventilation and air-conditioning) components. By applying this concept, they turned a standard 350 ton air-conditioning system into a 200 kW ORC power plant. The product is commercialised under the brand name PureCycle®280 by United Technologies Corporation (UTC). Plants based on this technology include East Hartford (CT), Austin (TX), Danville (IL) and Chena (Alaska). Binary units are also added to existing flash-steam plants to recover more power from hot, waste brine.

Regarding environmental impact, the only pollution of a binary plant is called thermal pollution (*DiPippo, 2016*). This is the amount of heat that must be rejected from the cycle in accordance with the laws of thermodynamics. In the case of a basic binary plant, the amount of thermal power that needs to be absorbed by the surroundings is about nine times the useful power delivered by the plant.

Selected binary cycle plants are listed in Tables 2-4 (*Tchanche et al., 2011; Zeyghami, 2015; Zarrouk and Moon, 2014*).

Table 2. Selected binary ORC geothermal power plants (Tchanche et al., 2011).

Plants/location	Resource temp. (°C)	Resource mass flow	Working fluid	Gross/net power (MW)	Thermal efficiency (%)
Amedee, USA	104	205 l/s	R-114	2.0/1.5	–
Wineagle, USA	110	63 l/s	Isobutane	0.75/0.6	–
Altheim, Austria	106	86 l/s	–	–/1.0	–
Otake, Japan	130	14.661 kg/s	Isobutane	–/1.0	12.9
Nigorikawa, Japan	140	50 kg/s	R-114	–/1.0	9.81
Reno, NV, USA	158	556 kg/s	Isobutane	27/21.744	10.2

Table 3. Examples of operating flash-binary geothermal power plants (Zeyghami, 2015).

Plants/location	Total capacity (MW)	Installed binary capacity (MW)
Brady, Nevada (USA)	20	5
Miravalles, Costa Rica	158	15.5
Leyte, Philippines	551	13.5
Mak-Ban, Philippines	458	15.7
Mokai, New-Zealand	111	18
Momotombo, Nicaragua	35	5
Svartsengi, Iceland	16.4	9.1
Wairakei, New Zealand	232	15
Puna, Hawaii (USA)	35	na

Table 4. Examples of binary power plants data (Zarroukand and Moon, 2014) T_{in} is the brine inlet temperature.

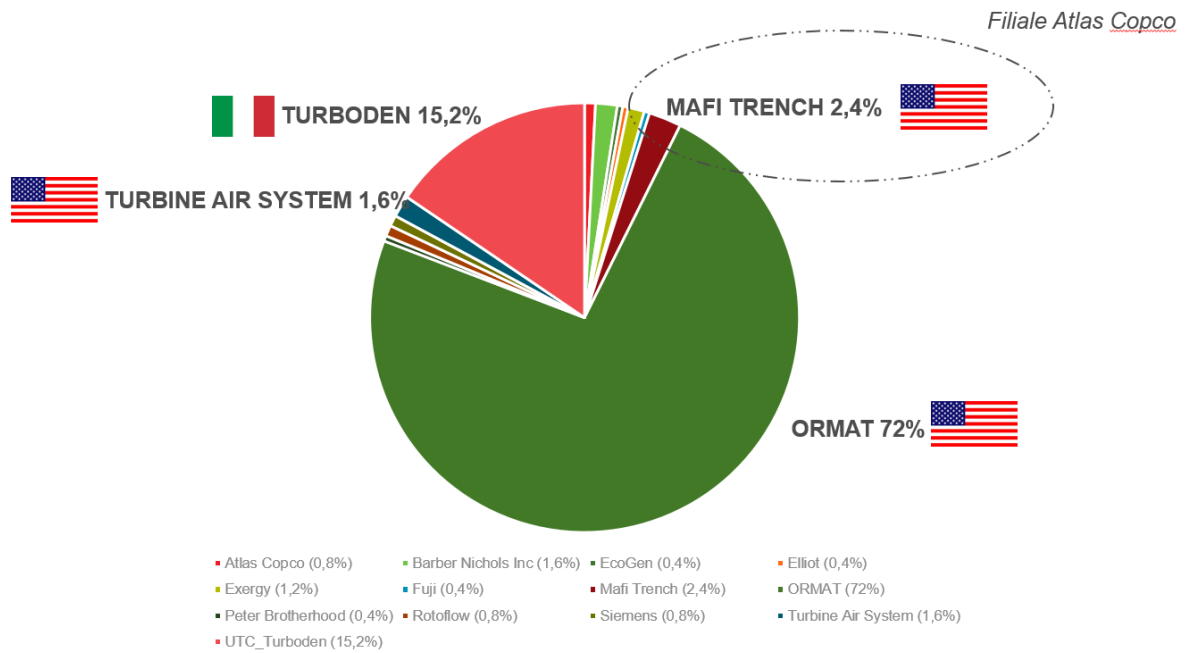
Country	Field (plant name)	No. unit	Start date	Installed capacity (MWe)	Running capacity (MWe)	\dot{m} (t/h)	T_{in} (°C)
USA	Alaska (Chena Hot Springs)	2	2006	0.5	0.4	471	73
USA	Wyoming-Casper (Rmotc-Ghcg)	1	2008	0.25	0.171	166	91
Germany	Neustadt-Glewe	1	2003	0.23	0.165	93	95
USA	Nevada (Wabuska)	3	1984	2.2	1.5	407	104
Australia	Altheim	1	2002	1	0.5	172	106
Australia	Blumau	1	2001	0.2	0.18	103	110
USA	California-Honey Lake (Wineagle)	2	1985	0.7	0.6	226	110
China	Nagqu	1	1993	1	1	300	112
Thailand	Fang	1	1989	0.3	0.175	28	116
Germany	Unter-Haching (Unter-Haching)	1	2009	3.36	3.36	424	120
USA	California-East Mesa (Ormesa IE)	10	1989	10	9	1054	136
USA	Idaho (Raft River)	1	2007	13	10	1440	140
USA	California-East Mesa (Ormesa 1)	26	1987	24	24	2652	147
Germany	Landau (landau)	1	2008	3	3	231	150
USA	California-East Mesa (Ormesa IH)	12	1989	12	10.8	935	153
USA	California-East Mesa (Ormesa 2)	20	1988	20	18	1555	154
France	Soultz-Sous-Forêts	1	2008	1.5	1.5	98	155
Nicaragua	Momotombo (Unit 3)	1	2002	7.5	6	628	155
USA	Nevada-Washoe (Steamboat 1,1A,2,3)	13	1986	35.1	31	6120	160
USA	California-Heber (Heber2)	12	1993	33	33.5	3266	166
Turkey	Salavatli	1	2006	7.4	6.5	545	170
USA	California-Casa Diablo (MP-1,2/LES-1)	10	1984	40	40	3240	175
Philippines	Makiling-Banahaw (Binary 1, 2, 3, 4)	6	1994	15.73	15.73	800	177
USA	Utah-Roosevelt Hot Springs (Blundell2)	1	2007	11	10	840	177
Mexico	Los Azufres (U-11,12)	2	1993	3	3	280	180
El Salvador	Berlin (U4)	1	2008	9.4	8	1018	185
USA	Nevada-Fallon (Soda Lake1)	3	1987	3.6	2.7	181	188
New Zealand	Northland (Ngawha)	2	1997	10	8	417	228
Japan	Oita (hatchobaru)	1	2006	2	2	82.1	246
New Zealand	Te Huka	1	2010	24	21.8	750	250
Portugal	Ribeira Grabde	4	1994	13	13	452	253

Kahraman *et al.* (2019) reviewed the geothermal power plants in Turkey (Table 5). Most of them are binary cycles (operated with n-pentane as working fluid).

Table 5. Geothermal power plants commissioned before 2013 in Turkey (Kahraman *et al.*, 2019).

GPP	Location	Installed Capacity (MWe)	Year	Type of the plant	The range of the brine temperature (°C)
Saraykoy	Denizli Kizildere	17.4	1984	Single flash	170–212
Dora 1	Aydin Salavatli	7.95	2006	Binary	165–176
Bereket	Denizli Kizildere	7.5	2007	Binary	195–212
Germencik	Aydin	47.4	2009	Double flash	205–215
Tuzla	Canakkale Tuzla	7.5	2010	Binary	150–171
Dora 2	Aydin Salavatli	9.5	2010	Binary	165–176
Irem	Aydin Hidirbeyli	20	2011	Binary	160–170
Sinem	Aydin	24	2012	Binary	160–180
Deniz	Aydin Bozkoy	24	2012	Binary	160–180
TOTAL		165.25			

In Indonesia, currently, there is only one commercially operational geothermal binary power plant, which is located in Sarulla, North Sumatra (Putera *et al.*, 2019, Pambudi, 2018). This binary system contributes as much as 49% of the total plant capacity of 110 MW. A smaller binary power plant with a capacity of 500 kW has been in development in Lahendong, North Sulawesi, since 2015, but it is not operational yet. Despite the potential, it is noted that there is still some reluctance to adopt binary power system technology, because the working fluids may have flammability and/or environmental issues. Another issue is the fact that binary power plants cannot contribute as much power as the main geothermal power plant, which might deter investors. The main binary-type systems manufacturers are illustrated in Figure 4. ORMAT is the main manufacturer for geothermal binary-type power plants. They supplied more than 70% of power units.



Source : IGA (2020)

Figure 4. Main binary system manufacturers.

4.2.3 Patents analysis

Patents from ORC manufacturers have been screened and the obtained corpus includes approximately 200 patents. This corpus has then been segmented into three groups according to (i) the heat exchanger technology (plate heat exchanger, shell & tube heat exchanger,...), (ii) the heat exchanger material (copper, titane, stainless steel, carbon steel,...), and (iii) the working fluid.

The graphs below illustrate the number of patent families for each manufacturer

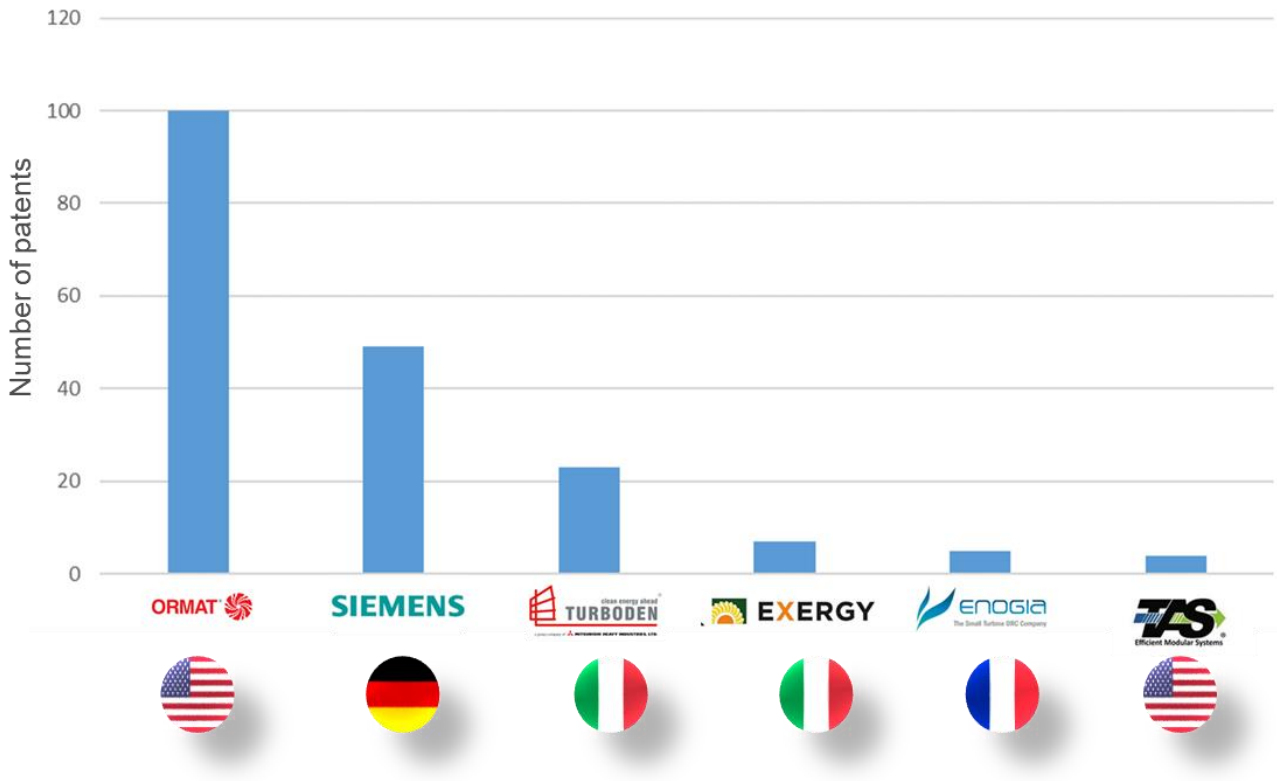


Figure 5: Inventive activity of main ORC manufacturers.

ORMAT (US) is the main applicant. It owns around 100 patents relating to heat exchangers for ORC geothermal units.

The temporal distribution of main applicants is illustrated in Figure 6. ORMAT and SIEMENS are core and longstanding applicants. EXERGY and ENOGIA own more recent patents.

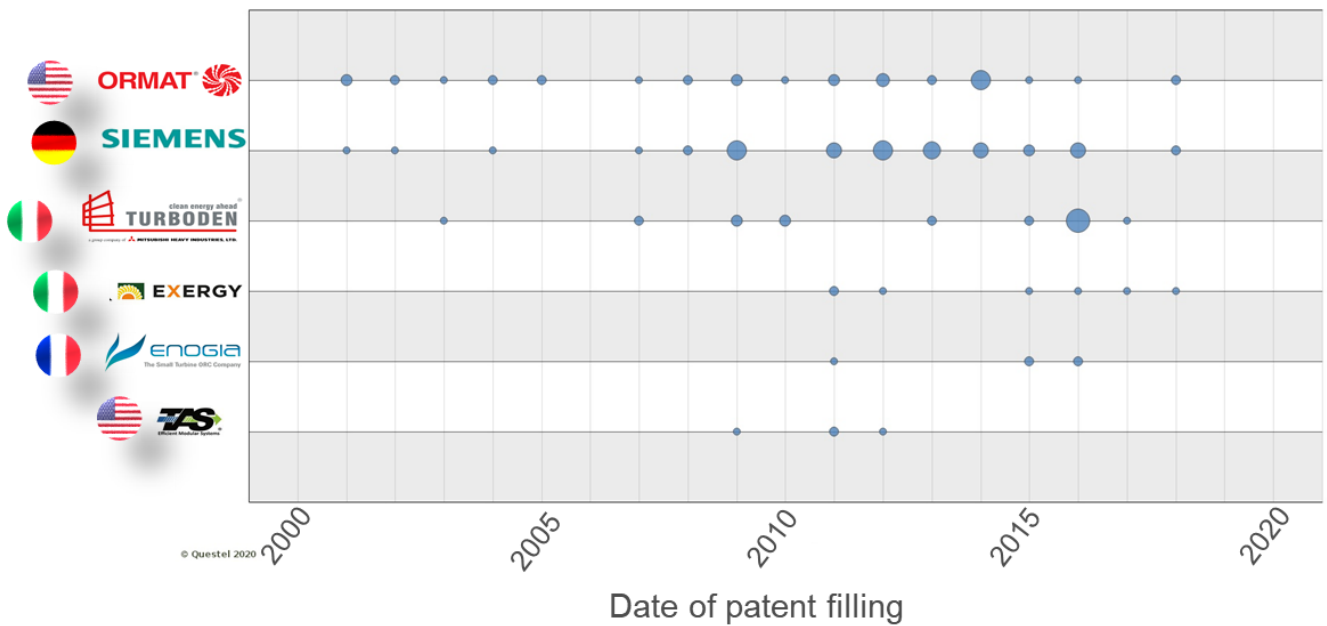


Figure 6: Date of patenting for each applicant.

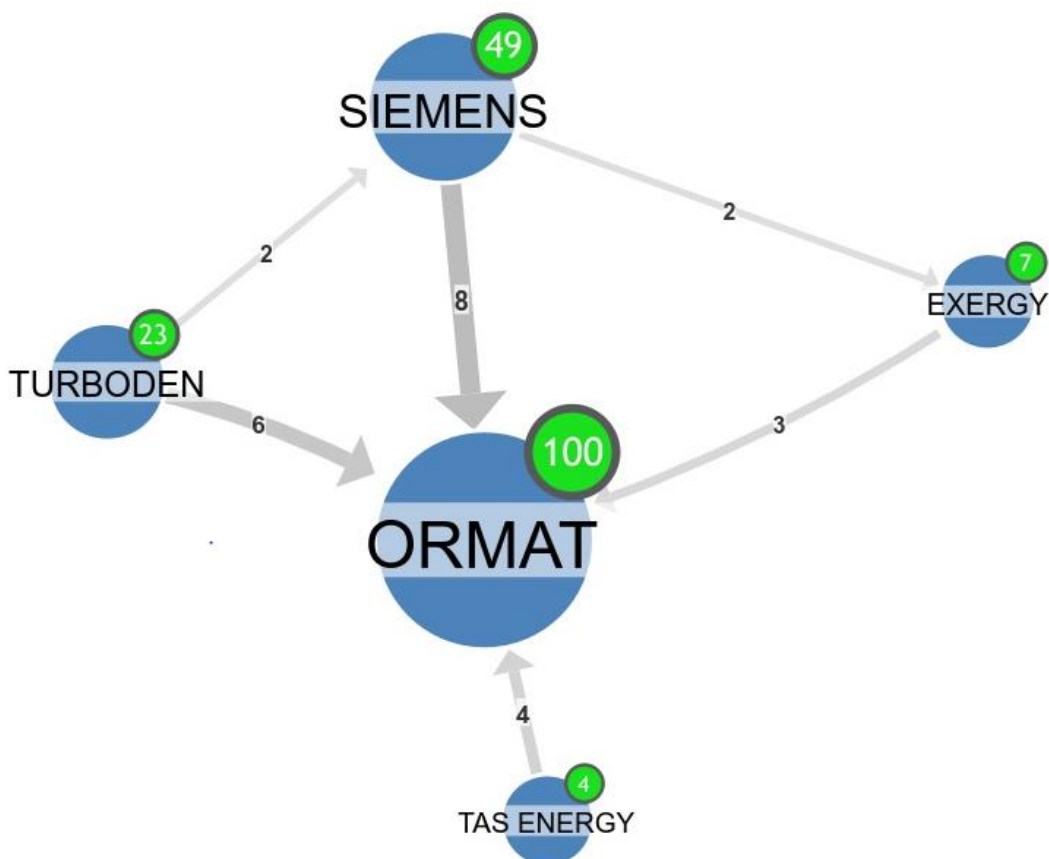


Figure 7: Patent citations between each applicant.

The main position of ORMAT is illustrated in Figure 7, which shows the citations between each applicant. ORMAT is often cited by other ORC manufacturers. Among the 100 patents, only 79 patents specify the heat exchanger technology and/or the working fluid. The heat exchanger material is only cited in 4 patents which is not enough to be relevant. The most cited working fluids and technology are respectively **alkanes** and **shell & tube heat exchanger**.

4.3 Organic Rankine Cycle

4.3.1 Working fluids

The selection of working fluids requires the consideration of the factors listed below (*Hung et al., 2010, Chen et al. 2010*):

- Toxicity of working fluid: all organic fluids are inevitably toxic. A working fluid with a low toxicity should be used to protect the personnel from the threat of contamination in case of a fluid leakage.
- Chemical stability: under a high pressure and temperature, organic fluids tend to decompose, resulting in material corrosion and possible detonation and ignition. Therefore a chemically-stable working fluid operated under appropriate working conditions should be selected.
- Boiling temperature: some of the organic fluids have a very low boiling temperature under atmospheric pressure. For those fluids, the temperature of cooling water in the condenser should be reduced. This can result in a more stringent requirement for the selection of the condenser.
- Flash point: a working fluid with a high flash point should be used in order to avoid flammability.
- Specific heat: a high value of specific heat represents a high load for the condenser. Hence a working fluid with a low specific heat should be used.

- Latent heat: a working fluid with a high latent heat should be used in order to raise the efficiency of heat recovery.
- Thermal conductivity: a high conductivity represents a better heat transfer in heat-exchange components.

Generally, organic fluids are heavy compounds with large molecular weights and low boiling temperatures and pressures. One of the most important ways to characterise the organic fluids is using the slope of their saturation vapor curve as shown in Figure 8 (Mahmoudi et al., 2018).

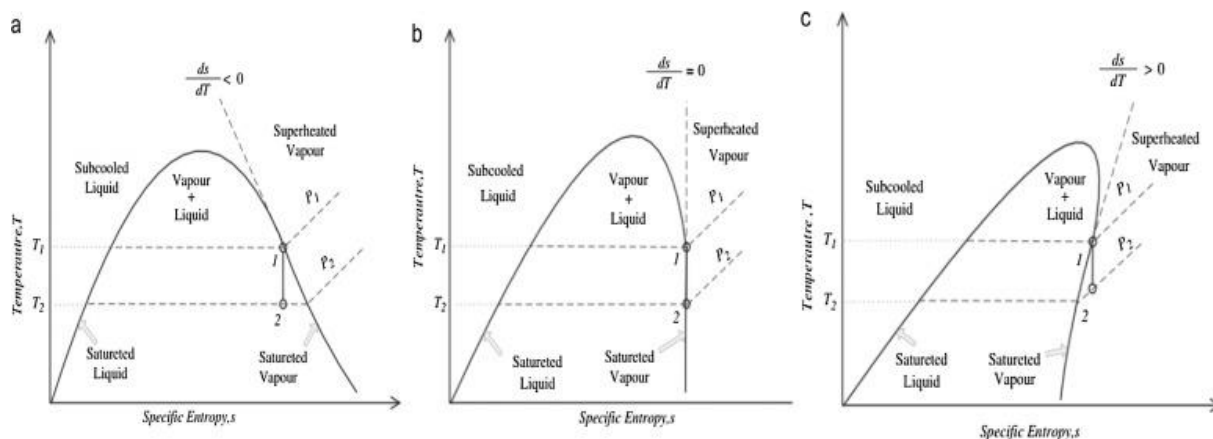


Figure 8. T–S diagram for (a) wet fluid, (b) isentropic fluid, and (c) dry fluid

Dry, wet and isentropic fluids have positive, negative and infinite slopes, respectively. For an ORC with lower operating temperatures, dry and isentropic fluids show better performances compared with wet fluids. For ORC systems with low-grade waste heat sources, organic fluids with lower latent heat of vaporisation show better thermal performance. Organic fluids with low specific volumes lead to smaller heat exchanger and expander sizes, reducing the size and cost of the system. It is better for cycle efficiency to have the critical temperature of the organic fluid close to the maximum temperature of the heat source. The freezing point of the organic fluid must be lower than the lowest temperature of the cycle. Higher molecular weight lowers the number of stages required for the expander which reduces the cost and complexity.

A selection of optimal working fluids according to the hot source temperature is listed in Table 6.

Table 6. The optimal working fluids in terms of net power output in different hot source (Mahmoudi et al., 2018).

Hot source temp. range (°C)	Working fluid
50–60	R23
65–70	Ethane
75–90	R7146
95–120	R218
125–160	R227ea
165–170	R124
175–185	R236ea
190	R245fa
195–200	Ipentane
205–235	Pentane
240–255	R123
260–280	R141b

Date: 31 March 2020

Haervig et al. (2016) and Vivian et al. (2015) provide guidelines to select the working fluids according to the ORC application and temperature level. Vivian et al. (2015) propose Table 7 that summarises the main thermodynamic and environmental properties of the selected working fluids: slope of the vapour saturation line (VSL) in the T - s diagram, critical temperature (T_{crit}) and pressure (p_{crit}), normal boiling temperature (NBT), GWP and safety level.

- *Vapor saturation line.* In general, dry (D) and isentropic (I) fluids are more appropriate than wet (W) fluids as they are superheated even after an isentropic expansion. So, the concerns of partial condensation in the final part of the turbine are eliminated.
- *Critical temperature.* A wide range of critical temperatures (from 71.9°C to 318.6°C) is considered in the exploitation of heat sources between 120°C and 180°C using different plant configurations (subcritical, supercritical).
- *Normal boiling temperature.* The table below shows that the normal boiling temperature approximately increases with critical temperature. Thus, it can be expected that the condensation pressure of fluids having a high critical temperature is lower than the atmospheric pressure.
- *Critical pressure.* A low critical pressure is desirable in order to limit the maximum pressure of the working fluid and consequently the costs for piping, sealing and equipment materials. Compared with other fluids, siloxanes and hydrofluoroethers (HFEs) show the lowest critical pressures. Different upper limits to cycle maximum pressure have been found in the literature: 60 bar, 44 bar or even 20 bar.
- *Global Warming Potential (GWP) and Ozone Depletion Potential (ODP).* Global Warming Potential is calculated over an atmospheric lifetime of 100 years and only fluids with ODP = 0 have been considered. HFCs are refrigerants that were introduced to replace HCFCs, which suffered a high ODP. Nonetheless, HFCs have high GWP (from hundreds to several thousand times higher than CO₂). Even higher is the GWP of PFCs. HFEs have more limited GWP. On the contrary, hydrocarbons and siloxanes have null (or very low) GWP. The problem of both these fluids is that they are highly flammable. This problem does not appear in other categories, such as HFEs, but their toxicity level could be dangerous due to the low exposure limits discovered in literature. The class of hydrofluoroolefins (HFOs) seems to best balance of safety and environmental concerns because of the low GWP, acceptable toxicity level and low flammability. With the above considerations being clear, the present work aims at finding general criteria for fluid selection and ORC optimisation based solely on thermodynamic considerations.
- *Safety level.* The safety level is indicated, according to the classification given by the ASHRAE Standard 34, by a character assessing the toxicity level (A = high toxicity, B = low toxicity) and a number assessing the flammability level (1 = no flame propagation, 2 = lower flammability, 3 = higher flammability).

Table 7. Properties of some working fluids (Haervig et al., 2016 and Vivian et al., 2015).

Fluid	Group	VSL	T_{crit} [°C]	NBT [°C]	p_{crit} [bar]	$GWP_{100\text{ yrs}}$	Safety level
R218	PFC	I	71.9	-24.3	45.2	8830	A1
RC318	PFC	D	115.2	-6.0	46.0	10300	A1
FC87	PFC	D	147.9	29.2	20.4	9160	
FC72	PFC	D	175.7	55.9	18.7	9300	
HFE7000	HFE	D	164.6	34.9	24.8	575	
HFE7100	HFE	D	195.3	59.6	22.3	297	
HFE7500	HFE	D	261.0	127.9	15.5		
R143a	HFC	W	72.7	-47.5	37.6	4470	A2
R32	HFC	W	78.1	-51.9	57.8	675	A2
R134a	HFC	I	101.1	-26.1	40.6	1430	A1
R227ea	HFC	D	101.6	-16.4	29.0	3220	A1
R152a	HFC	W	113.3	-24.3	45.2	124	A2
R236fa	HFC	D	124.9	-1.8	32.0	9810	A1
R245fa	HFC	I	154.0	14.9	36.5	1030	B1
R1234yf	HFO	I	94.7	-29.8	33.8	4	A2L
R1234ze	HFO	I	109.4	-19.6	36.3	6	A2L
Propane	HC - Alkane	W	96.7	-42.4	42.5	0	A3
Isobutane	HC - Alkane	D	135.0	-12.2	36.5	0	A3
Butane	HC - Alkane	D	152.0	-0.9	38	0	A3
Isopentane	HC - Alkane	D	187.2	27.5	33.7	0	A3
Pentane	HC - Alkane	D	196.5	35.5	33.6	0	
Hexane	HC - Alkane	D	234.7	68.8	30.6	0	
Heptane	HC - Alkane	D	267.0	97.9	27.3	0	
Cyclohexane	HC - Alkane	D	280.5	80.3	40.7	0	
Octane	HC - Alkane	D	296.2	125.0	25.0	0	
Propylene	HC - Alkene	W	92.4	-48.0	46.6	2	A3
Benzene	Aromatic HC	D	288.9	79.6	48.9		
Toluene	Aromatic HC	D	318.6	109.9	41.3	0	
HMDS	Linear SX	D	245.5	99.8	19.4		
OMTS	Linear SX	D	290.9	152.1	14.1		
D4	Cyclic SX	D	313.3	174.9	13.3	<20	

Unverdi and Cerci (2013), Table 8, and Franco (2011), Table 9, listed a few binary cycles with their associated working fluid and power production quantity.

Table 8. Binary cycles and power production quantity which can be established in accordance with the studied power plant (Unverdi and Cerci, 2013).

Plant and location	Geothermal temperature (°C)	Cycle	Working fluid	Gross capacity (kWe)	Specific brine consumption (kg/s)/MW	Compatible with Germencik Geothermal Power Plant (MWe)
Kutahya-Simav, Turkey	145	Rankine with superheat	R124	2900	42	37.39
Nigorikawa, Japan	140	Rankine	R114	1000	50	10.83
Otake, Japan	130	Rankine	Isobutane	1000	14.7	36.85
Husavik, Iceland	124	Kalina	NH ₃ -H ₂ O	1700	53	17.37
Wineagle, USA	110	Rankine	Isobutane	700	63	6
Nagqu, China	110	Rankine	Iso-pentane	1000	69	7.85
Altheim, Austria	106	Rankine	C ₅ F ₁₂	1000	86	6.23
Wabuska, CA, USA	104	Rankine	Iso-pentane	1750	34.3	27.64
Neustadt-Glewe, GER	98–100	Rankine	C ₅ F ₁₂	230	120.8	1.03
Birdsville, Australia	98–99	Rankine	R114	150	200	0.41
Chena Hot Spring, AK, USA	74	Rankine	R134a	400	57.9	3.74

Table 9. Small binary power plants using low-temperature geothermal resources or non-conventional working fluids (Franco, 2011).

Plant and location	T_{geo} (°C)	Cycle	Working fluid	Gross capacity (kWe)	Specific brine consumption [(kg/s)/MW]	Cooling tower
Husavik, Iceland	124	Kalina	NH ₃ -H ₂ O	2030 (1700)	53	Wet
Unternhaching, GER	122	Kalina	NH ₃ -H ₂ O	4000 (3400)	44.2	Wet
Bruchsal, GER	120	Kalina	NH ₃ -H ₂ O	610 (550)	51.8	Wet
Empire, USA	118	RAN	Isopentane	1200 (1000)	90.8	Dry
Fang, Thailand	116	RAN	Isopentane	300 (175)	47.4	Wet
Nagqu, China	110	RAN	Isopentane	1300 (1000)	69	Dry
Bad Blumau, Austria	110	RAN	Isopentane	250 (180)	120	Dry
Wineagle (Susanville), USA	110	RAN	Isobutane	750 (600)	105	Dry
Altheim, Austria	106	RAN	C ₅ F ₁₂	1000 (500)	86	Dry
Wabuska, USA	104	RAN	Isopentane	750 (600)	90	Wet
Wendel, USA	103	RAN	R114	2000 (1600)	128.2	Wet
Birdsville, Australia	98–99	RAN	R114 (Isopentane)	150 (120)	200	Wet
Neustadt-Glewe, GER	98–100	RAN	C ₅ F ₁₂	230 (180)	120.8	Wet
Chena Hot Spring, USA	74	RAN	R134a	250 (210)	57.9	Wet/dry

The plants reported in Table 9 (Franco, 2011) cover a wide range of geothermal fluid temperatures (74–124°C) so that brine specific consumption, which is strongly dependent on the thermodynamic and chemical properties of the geofluid, lies in the range from 44 to 200 kg/s for each MW of electricity produced. The remarkable difference among the various plant performances can be explained in a lot of cases with the differential temperature between source temperature and rejection temperature.

Despite the extensive research conducted for selection methodologies and operating characteristics of working fluids for various ORC applications, only a few working fluids are used in commercial ORC applications. Tables 10 and 11 shows the list of some well-known ORC system manufacturers, their working fluid, and heat source temperature (Imran et al., 2016; Tomarov and Shipkov, 2017).

Table 10. ORC manufacturers and their system configuration (Imran et al., 2016).

Manufacturer	Working fluid	Heat source temperature
Atlas Copco	Hydrocarbons	200–300 °C
Adoratec GmbH/Maxxtec AG	OMTS	320 °C
Bosch KWK GmbH	R-245fa	>140 °C
Calnetix Technologies LLC	R-245fa	>95 °C
Conpower	SES36	>85 °C
Cryostar SAS (Linde Group)	R-245fa, R-134a	N/A
Cryotec Anlagenbau GmbH	OMTS, Hydrocarbons	120 °C
Dürr Cyplan	Hydrocarbons	90–1000 °C
DeVeTec GmbH	Ethanol	300–600 °C
ElectraTherm Inc.	R-245fa	77–116 °C
Eneftech Innovation SA	R-245fa	125–200 °C
E-Rational	R-245fa, SES36	80–150 °C
Exergy (Maccaferri Industrial Group)	Pentane, Isopentane,	90–300 °C
Freepower	Hydrocarbons	N/A
GE Clean Cycle	R-245fa	>155 °C
GMK (Germany)	GL160 (patented)	<300 °C
Infinity Turbine LLC	R-134a, R-245fa	80–140 °C
LTi Reenergy	N/A	>160
Opcon	Ammonia	55–250 °C, >250 °C
Orcan Energy GmbH	N/A	N/A
Ormat Technologies Inc.	n-pentane	150–300
PureCycle	R-245fa	91°C–149 °C
TAS Energy	R-134a, R-234fa, R-245fa	97–260 °C
Tri-o-gen	Toluene	>350 °C
Turboden	OMTS, Solkatherm	100–300 °C

Table 11: Characteristics of binary plants’ equipment (Tomarov and Shipkov, 2017).

Manufacturer	Unit capacity, kW	Heat source temperature, °C	Technological features	
			working fluid	turbine
ORMAT, United States	200–70 000	150–300	n-Pentane	Two-stage axial
Turboden, Italy	200–2000	100–300	OMTS	As above
GMK, Germany	50–5000	120–350	–	Multistage axial
Turboden Pure Cycle, United States	280	91–149	R245fa	Radial
Cryostare, France	–	100–400	R-245fa, R-134a	”
Infinity Turbine, United States	10–50, More than 250	Less than 90, 90–120	R-134a, R-245fa	–
Barber Nichols, United States	700, 2000, 2700	More than 115	–	–
Trans Pacific Energy, United States	100–5000	30–480	Mixture of organic compounds	–
Kaluga Turbine Plant, Russia	2500	More than 100	R-134a	Single-stage radial-axial

For low and mid-range heat source temperatures (<150-200°C), **R134a and R245fa** seem preferred. **OMTS, pentane and toluene** are preferred for high heat source temperatures (>200-300°C, Imran et al. 2016). According to Tomarov and Shipkov (2017), of over 300 chemical compounds that theoretically can be used in a binary plant cycle, only approximately 15 organic substances and mixtures having a low boiling point are used.

In 2017, geothermal binary power units, which use various organic compounds as a working fluid were as shown in Table 12.

Table 12 : Distribution of the working fluids used in geothermal binary power plants (% of the total installed capacity of binary cycle power units in the world, (Tomarov and Shipkov, 2017).

Hydrocarbons	82.7
Fluorocarbons	6.7
Chlorofluorocarbons	2.0
Ammonia–water mixture	0.5
Data on the working fluid is n/a	8.2

In 2017 (Tomarov and Shipkov, 2017), the generating capacity of binary power units running on hydrocarbons was equal to approximately 82.7% of the total installed capacity of all the binary power units in the world. Relatively cheap hydrocarbons (pentane, isobutane, isopentane, etc) characterised by good thermodynamic and thermal properties are explosive and flammable and can be used in open type power plants, which is not always acceptable to the areas with negative winter temperatures (Tomarov and Shipkov, 2017).

Zeyghami (2015) performed thermodynamic calculations to compare working fluid efficiencies (Table 13). The condensing temperature is assumed to be 30°C. Calculations have been performed for a geofluid temperature range between 150°C and 250°C. Also, to eliminate the scaling problems in the piping system and evaporator heat exchanger, the minimum geofluid temperature is set to 70°C.

Table 13. Performance parameters for several working fluids for combined flash-binary cycle (Zeyghami, 2015).

Working fluid	T_1 [°C]	I^*	VER	$\dot{W}_{T,s}$ [kJ/kg]	$\dot{W}_{T,b} - \dot{W}_{P,b}$ [kJ/kg]	Overall first law efficiency (η)	Overall second law efficiency (ϵ)
R152-a	150	0.520	6.67	10.31	31.75	0.080	0.480
R124	150	0.521	10.19	8.88	32.73	0.080	0.479
R-236fa	150	0.525	7.24	8.74	33.2	0.079	0.475
R-C138	150	0.533	10.20	15.68	25.22	0.078	0.467
Isobutane	150	0.536	5.76	6.12	34.53	0.077	0.464
Butane	200	0.445	14.96	25.86	64.10	0.120	0.554
Trans-butene	200	0.449	13.92	17.96	71.25	0.119	0.550
Isobutene	200	0.451	10.97	33.63	55.26	0.119	0.548
Butene	200	0.452	10.72	31.15	57.65	0.119	0.547
Propyne	200	0.452	8.36	41.03	47.76	0.119	0.547
Cis-butene	250	0.418	14.88	78.15	71.7	0.153	0.583
Trans-butene	250	0.425	13.92	85.39	62.63	0.151	0.575
Butane	250	0.431	14.96	87.30	59.22	0.149	0.570
Butene	250	0.441	10.72	88.14	55.88	0.147	0.560
Isobutene	250	0.443	10.97	88.77	54.71	0.146	0.558

The results regarding the working fluids showed that:

- For geofluid temperature equal to 150°C, in terms of I^* (dimensionless exergy losses) and VER (vapor expansion ratio), R152-a, R124, R-236fa, R-C138, and isobutane are shortlisted as the top five working fluids.
- For geofluid temperature equal to 200°C, in terms of I^* and VER, Butane, Trans-butene, Isobutene, Butene, and Propyne are shortlisted as the top five working fluids.
- For geofluid temperature equal to 250°C, in terms of I^* and VER, Cis-butene, Trans-butene, Butane, Butene, and Isobutene are shortlisted as the top five working fluids.
- At low geofluid temperatures ($150^\circ\text{C} \leq T_1 < 200^\circ\text{C}$), using **refrigerants** as the ORC working fluid results in slightly higher performance than hydrocarbons. But at high temperatures ($200^\circ\text{C} \leq T_1$), hydrocarbons are more suitable choices.

Saleh et al. (2007) screened 31 pure component working fluids for organic Rankine cycles for geothermal applications (heat source around 100°C). The fluids are alkanes, fluorinated alkanes, ethers and fluorinated ethers. Two plant examples are cited: (i) Altheim, Austria (1 MWe) and (ii) Neustadt-Glewe, Germany (0.2 MWe) both of which used **n-perfluoropentane** as working fluid.

Date: 31 March 2020

Eyerer et al. (2020) reported the data of existing plants for power production from hydrothermal geothermal reservoirs in Germany. They reviewed seven ORC cycle architectures that were commissioned between 2007 and 2016. They are all equipped with air-cooled condensers. The manufacturers are Turboden srl, Ormat Technology Inc. and Intec GMK GmbH. The working fluids with their respective wellhead temperatures are R600a (127°C), R601a (165°C), R245fa (140°C) and R134a (118°C) for the most recent plant (2016).

Finally, the most common working fluids seem to be **n-pentane**, **isopentane** and **R245fa**. Their advantages are (Zare, 2015) :

- High latent and specific heat
- High density in both liquid and gas phase
- Moderate critical temperature and pressure
- Moderate evaporating and condensing temperatures.
- Excellent transport and heat transfer properties
- Safety and chemical stability
- Material capability and no corrosion
- Market availability and low cost
- Environmentally benign

From the patents analysis, **alkanes** are the most cited working fluid among the 100 patents relative to heat exchangers in ORC units. They have been used since 1980. **Siloxanes** appeared in patent descriptions in 2004, **fluorocarbons** in 2008 and **hydrofluoroolefin** in 2013 probably because of the evolution of the legal context regarding refrigerants.

4.3.2 Operating data – Case studies

Recently, the thermo-economic approach has been increasingly popular and most scientific articles concern thermo-economic evaluations and energy/exergy calculations. However, to validate the models, several case studies are reported in the literature and the authors need real operating conditions. This section reports the several case studies and the associated operating data (generated power, operating temperatures and pressures, brine temperature, condensation mode, working fluid, heat exchangers, etc). It is worth noting that for optimisation calculations, the ratio of the total heat exchanger area to net power output is mainly used as the objective function (cost-effective optimum design) (Hettiarachchi et al., 2007; Kanoglu and Bolatturk, 2008; Putera et al. 2019; Budisulistyo and Krumdieck, 2015; Mendrinós et al., 2006).

DiPippo (2004) reviewed several binary cycles to perform second law analyses:

- Otake pilot binary geothermal power plant:
Otake, on the Japanese island of Kyushu, was the site of one of the most intriguing geothermal binary power plants. The plant had a rated power of 1000 kW and received both steam and brine from the adjacent 10 MW Otake flash-steam plant. It used a unique 18-stage flash evaporator to efficiently heat **isobutane**, the cycle working fluid (see Figure 9). The relevant plant data are given in Table 14.

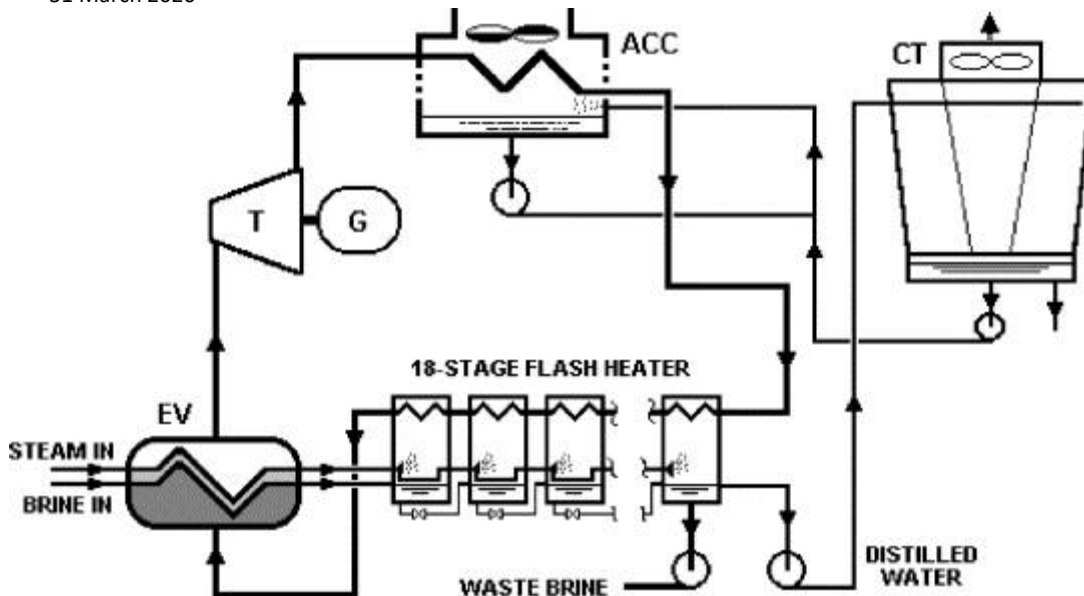


Figure 9. Otake pilot binary plant. ACC: air-cooled condenser; CT: cooling tower; EV: evaporator; G: generator; T: turbine.

Table 14. Operating data for Otake pilot binary plant.

Item	Data
Steam inlet temperature (°C)	130
Steam flow rate (kg/s)	1.305
Brine inlet temperature (°C)	130
Brine flow rate (kg/s)	13.356
Geofluid flow rate (total) (kg/s)	14.661
Geofluid outlet temperature (°C)	50
Plant rated power (kW)	1000
Dead-state temperature (°C)	18

The extremely efficient 18-stage flash evaporator is a key to the high performance (exergy conversion efficiency of 53.9%). As a footnote, this plant was tested and then dismantled. No plant of a similar design has ever been built again, most likely indicating that the economics were unfavourable.

- Nigorikawa binary geothermal power plant:

Another pilot binary plant, the Nigorikawa (or Mori) plant, was built by the Japanese near Hakodate on Hokkaido, contemporaneously with the Otake pilot plant. This plant also was rated at 1000 kW but used a simple binary cycle. The plant incorporated a two-stage condenser, which is not shown in the simplified schematic (Figure 10).

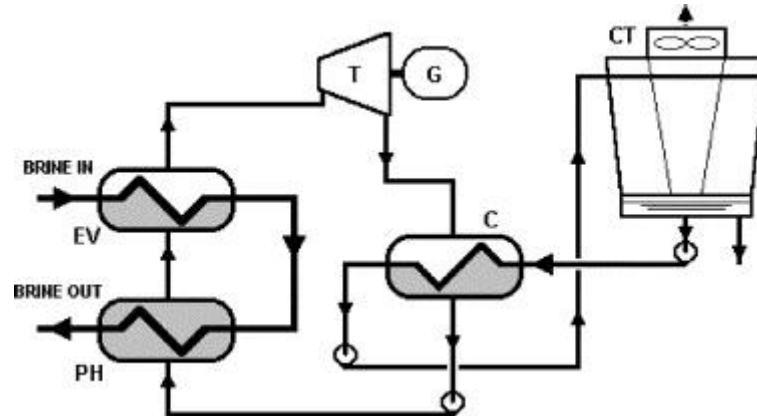


Figure 10. Nigorikawa (Mori) binary plant. C: condenser; PH: preheater.

The cycle working fluid was **Refrigerant-114 (C₂Cl₂F₄)**. Table 15 gives the specifications.

Table 15. Operating data for Nigorikawa binary plant

Item	Data
Brine inlet temperature (°C)	140
Brine outlet temperature (°C)	92
Brine flow rate (kg/s)	49.996
Plant rated power (kW)	1000
Dead-state temperature (°C)	13

In contrast with the high-efficiency Otake binary plant, the Nigorikawa unit had exergetic and thermal efficiencies typical of binary plants (exergy conversion efficiency of 21.6%). Like the Otake pilot plant, the Nigorikawa plant was also dismantled after its test period was concluded.

- Heber SIGC geothermal power plant:

A multi-unit advanced binary plant has been in operation at the Heber geothermal field in the Imperial Valley, California, since June 1993. The plant consists of six integrated dual-level units. Brine is pumped from the reservoir and arrives at the plant at a temperature of 165°C, somewhat higher than for a typical “low-temperature” plant. A simplified schematic is shown in Figure 11.

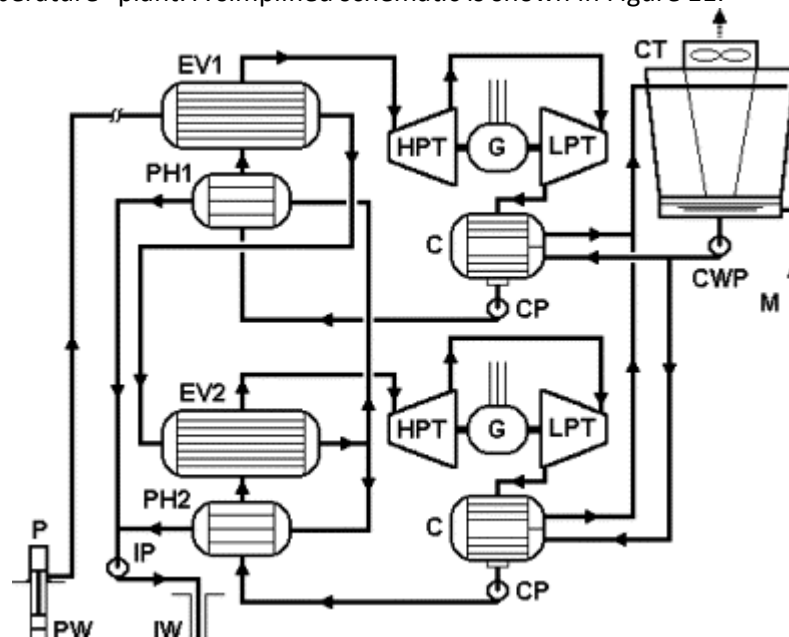


Figure 11. Simplified schematic of Heber SIGC power plant. CP: condensate pump; CWP: cooling water pump; HPT, LPT: high-, low-pressure turbine; IP: injection pump; IW: injection well; P: pump; PW: production well.

The working fluid is **isopentane**. Preheaters, evaporators and condensers are **shell-and-tube heat exchangers**. Their respective heat duty is 9 W, 18 MW and 23 MW. **Water-cooled condensers** are used with an inlet water temperature of 20°C (DiPippo, 2016).

- Húsavík Kalina cycle power plant:
The Kalina KCS-34 binary power plant at Húsavík, Iceland, is shown in simplified schematic form in Figure 12.

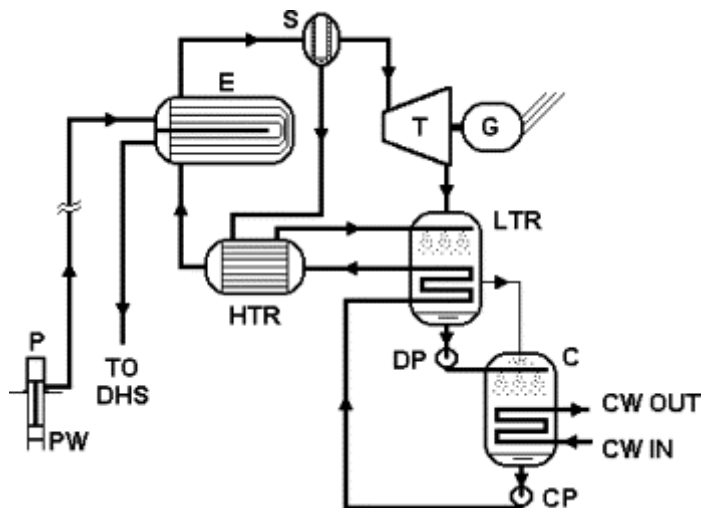


Figure 12. Simplified schematic of Húsavík power plant. CW: cooling water; DHS: district heating system; DP: drain pump; E: evaporator; HTR, LTR: high-, low-temperature recuperator.

Operating data are given in Table 16. The working fluid is a mixture of 82% ammonia and 18% water. This composition was optimised to match the temperature of the brine stream (121°C).

Table 16. Operating data for the Húsavík plant

Item	28 November 2001	29 November 2001
Brine flow rate (kg/s)	90 (design)	90 (design)
Brine inlet temperature (°C)	122	121
Cooling water flow rate (kg/s)	182 (design)	202 (111% design)
Cooling water inlet temperature (°C)	5 (design)	5 (design)
Gross electric power (kW)	1823	1836
Auxiliary power (kW)	127	127
Net electric power (kW)	1696	1709

- Brady bottoming binary cycle
The final case study of DiPippo’s review (2004) is the bottoming binary cycle installed as part of the Brady Hot Springs double-flash power plant (Figure 13). Operating data are given in Table 17. A simple binary plant recovers waste heat from the spent brine leaving the low-pressure flash vessels.

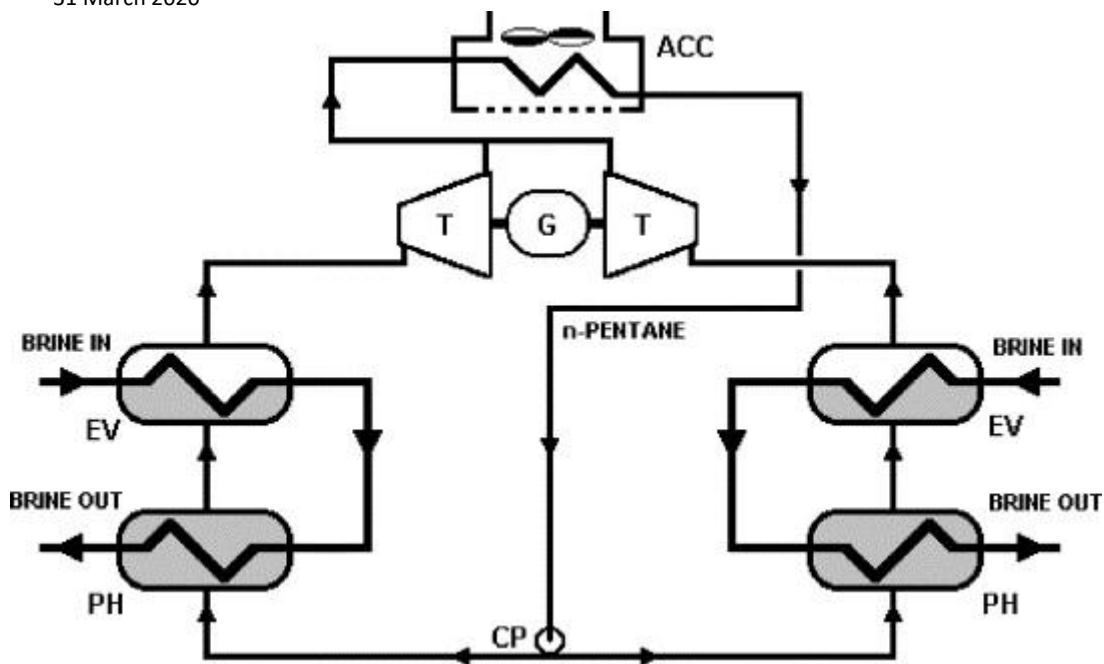


Figure 13. Brady bottoming binary cycle.

Table 17. Averaged data for Brady bottoming binary cycle: 16–25 September 2002

Item	6:00 a.m.	Range	6:00 p.m.	Range
Brine inlet temperature (°C)	107.8	106.0–109.0	108.7	105.9–109.3
Brine outlet temperature (°C)	81.11	79.7–82.7	83.32	82.2–84.6
Brine flow rate (kg/s)	484.09	474.3–489.7	484.09	474.3–489.7
Ambient temperature (°C)	16.8	11.1–23.3	30.1	24.4–35.6
Gross power (kW)	5.21	4.5–6.0	3.78	3.0–4.7
Auxiliary power (kW)	0.88	Constant	0.88	Constant
Net power	4.33	3.7–5.2	2.90	2.2–3.9

Geothermal binary plants are relatively poor converters of heat into work. First Law or thermal efficiencies typically lie in the range of 8–12%. As a consequence, a 1–2 percentage point improvement in power output translates into a gain of about 10–20% in efficiency.

The results of second-law analysis by *DiPippo (2004)* show that binary plants can operate with very high Second Law or exergetic efficiencies even when the motive fluids are low-temperature and low-exergy. Exergetic efficiencies of 40% or greater have been achieved in certain plants with geofluids having specific exergies of 200 kJ/kg or lower. The main design feature leading to a high Second Law efficiency lies in the **design of the heat exchangers** to minimise the loss of exergy during the heat transfer processes. Another important feature that can result in a high Second Law efficiency is the **availability of low-temperature cooling water** that allows a once-through system for waste heat rejection.

The geothermal power plant analysed by *Kanoglu and Bolatturk (2008)* is a binary design plant (geothermal power plant in **Reno, NV, USA**) that generates a yearly average net power output of about 27 MW. The plant consists of two identical units, each having two identical turbines. A schematic of one unit is given in Figure 14. The power plant operates on a liquid-dominated resource at 160°C. The brine passes through the heat exchanger system that consists of a series of **counter-flow heat exchangers** where heat is transferred to the working (binary) fluid **isobutane** before the brine is reinjected back to the ground. Superheated isobutane is generated at the heat exchanger exit. An equal amount of isobutane flows through each turbine. It utilises a **dry-air condenser** to condense the working fluid, so no fresh water is consumed. Isobutane circulates in a closed cycle, which is based on the Rankine cycle.

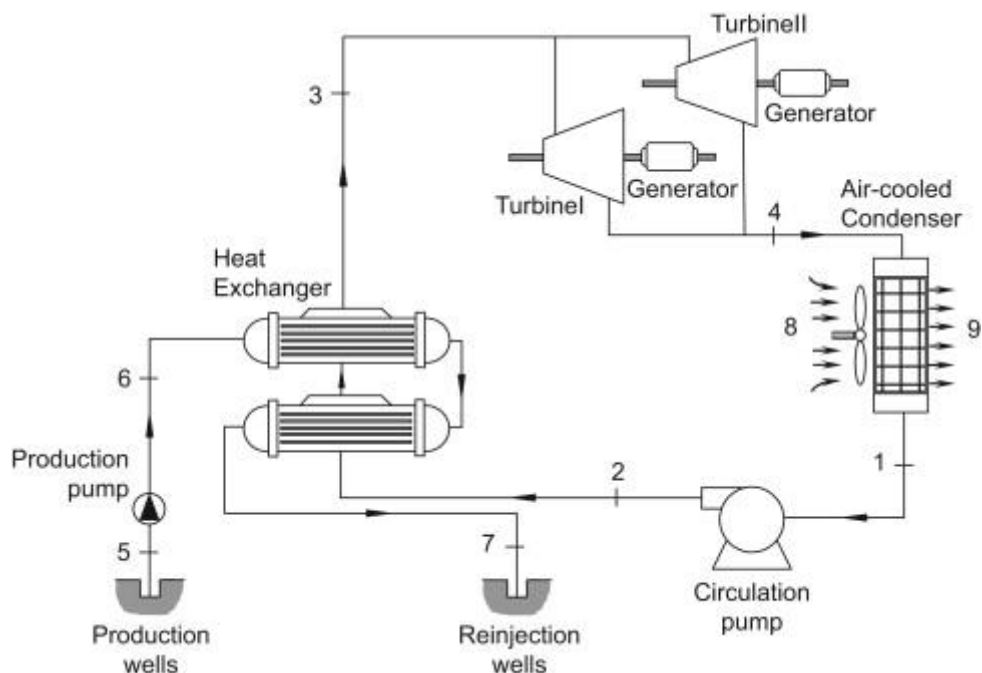


Figure 14. Schematic layout of the plant.

The authors do not specify the heat exchanger technology but according to the schematic layout, the preheater and the evaporator seem to be **shell and tube heat exchangers**.

The harvested geothermal fluid is saturated liquid at 160°C and 1264 kPa in the reservoir. The heat source for the plant is the flow of geothermal water (brine) entering the plant at 158°C and 609 kPa with a total mass flow rate of 555.9 kg/s. Geothermal fluid remains as a liquid throughout the plant. The brine leaving the heat exchangers is directed to the reinjection wells where it is reinjected back into the ground at 90°C and 423 kPa. In the plant, a mass flow rate 305.6 kg/s of working fluid circulates through the cycle. The working fluid enters the heat exchanger at 13.7°C and leaves after it is evaporated at 128°C and superheated to 146.8°C. The working fluid then passes through the turbines that each have mass flow rate of 152.8 kg/s. It exhausts to an **air-cooled condenser** at about 79.5°C where it condenses to a temperature of 11.7°C. Approximately, 8580 kg/s air at an ambient temperature of 3°C is required to absorb the heat yielded by the working fluid. This raises the air temperature to 19.4°C. The working fluid is pumped to heat exchanger pressure to complete the Rankine cycle. The exergetic efficiencies and effectiveness of the heat exchanger are 80.5% and 47.1%, respectively. This exergetic efficiency can be considered to be high, and indicate a satisfactory performance of the heat exchange system.

Kanoglu (2002) also analysed a binary design plant that generates 12.4 MWe net electricity from seven identical paired units (Stillwater binary geothermal power plant located in **Northern Nevada, USA**). Full power production started in April 1989. The plant operates in a closed loop with no environmental discharge and 100% reinjection of geothermal fluid. The modular power plant operates on a liquid-dominated resource at 163°C. It utilises dry-air condensers to condense the working fluid, so no fresh water is consumed. The geothermal field includes four production wells and three reinjection wells. The plant uses **isopentane** as the working (binary) fluid. Isopentane circulates in a closed cycle, which is based on the Rankine cycle.

The schematic layout of the plant in Figure 15 shows only one representative unit (among a total of seven paired units). The heat source for the plant is the flow of geothermal water (brine) entering the plant at 163°C with a total mass flow rate of 338.94 kg/s (48.42 kg/s mass flow rate for each unit). Geothermal fluid remains as a

liquid throughout the plant. The brine exits at around 65°C. The brine leaving the preheaters is directed to the reinjection wells where it is reinjected back into the ground.

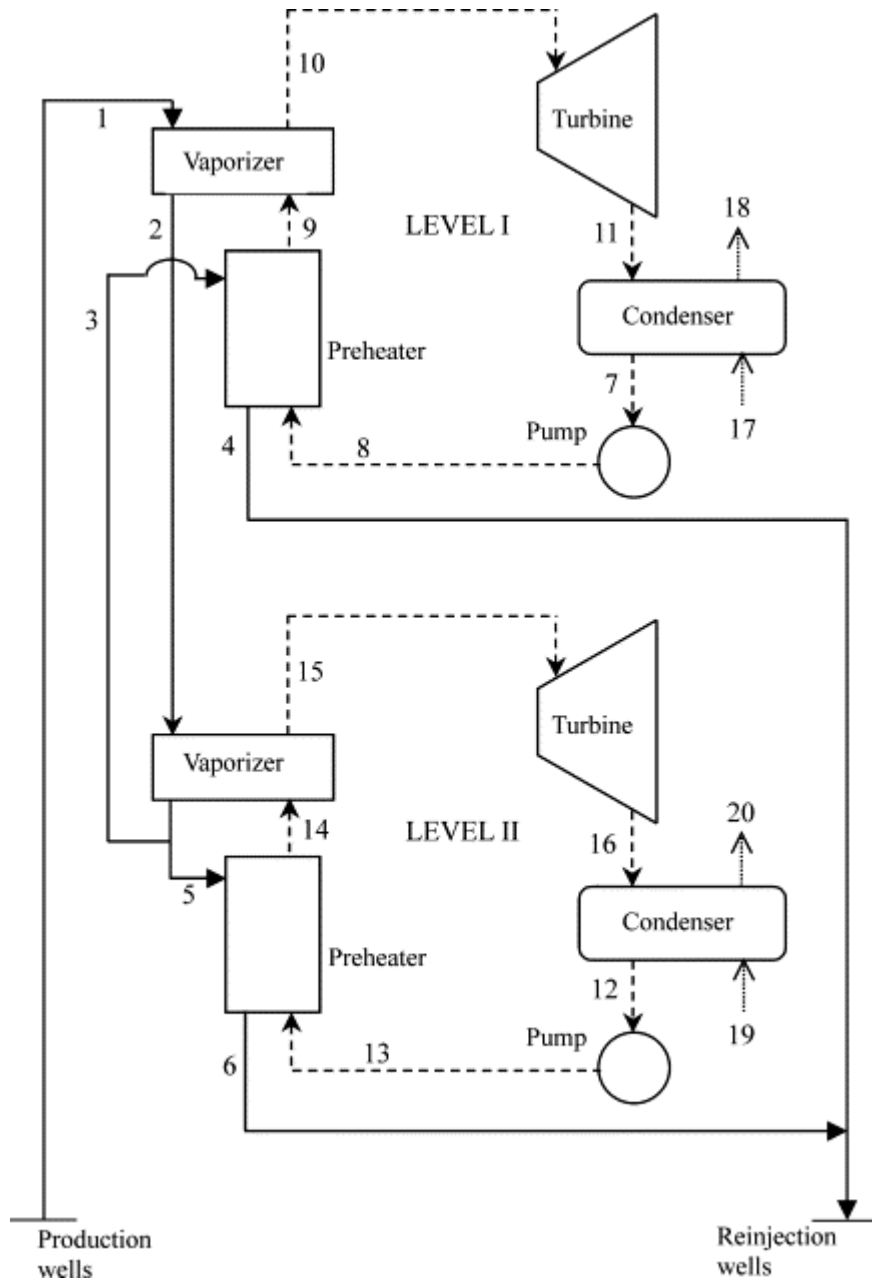


Figure 15: Schematic layout of the Stillwater binary geothermal power plant.

In Level I (Figure 16), 19.89 kg/s of working fluid circulates through the cycle. The working fluid enters the preheater at 32°C and leaves at about 98°C. It then enters the vaporiser where it is evaporated at 133°C and superheated to 136°C. The working fluid then passes through the turbine. It exhausts to an air-cooled condenser at about 85°C where it condenses to a temperature of 31°C. Approximately 530 kg/s air at an ambient temperature of 13°C is required to absorb the heat yielded by the working fluid. This raises the air temperature to 29°C.

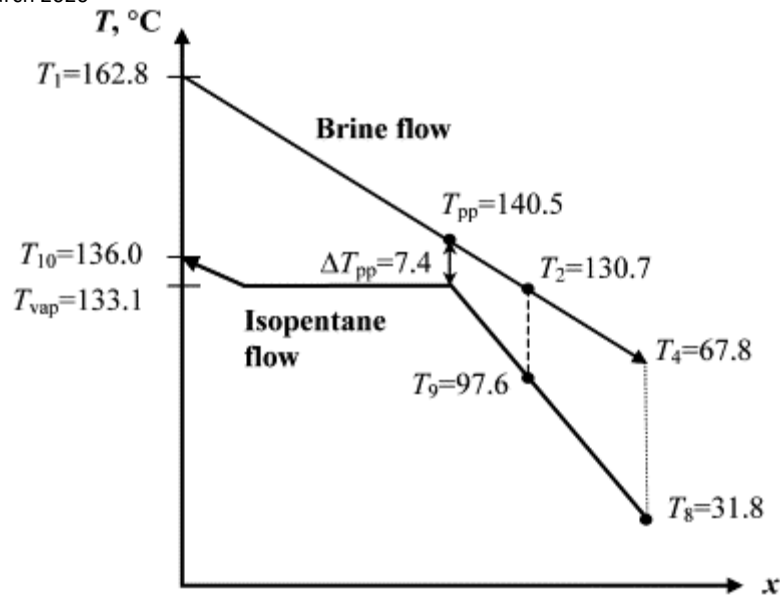


Figure 16. Diagram showing the heat exchange process between the geothermal brine and the working fluid isopentane in Level I. The x-axis represents the path of the fluid flow in the heat exchanger.

Moya and DiPippo (2007) describe the adding of an extra unit on the geothermal site of **Miravalles (Costa Rica)**. This concerns a binary cycle unit (ORC from Ormat Inc.). The brine temperature is around 165°C and the working fluid is **pentane**. This unit was commissioned in January 2004. The brine outlet temperature is between 138 and 133°C which leaves a 5°C margin of safety to avoid silica saturation and scaling issues. The simplified flow diagram for one of the two converters of the additional ORC unit is depicted in Figure 17:

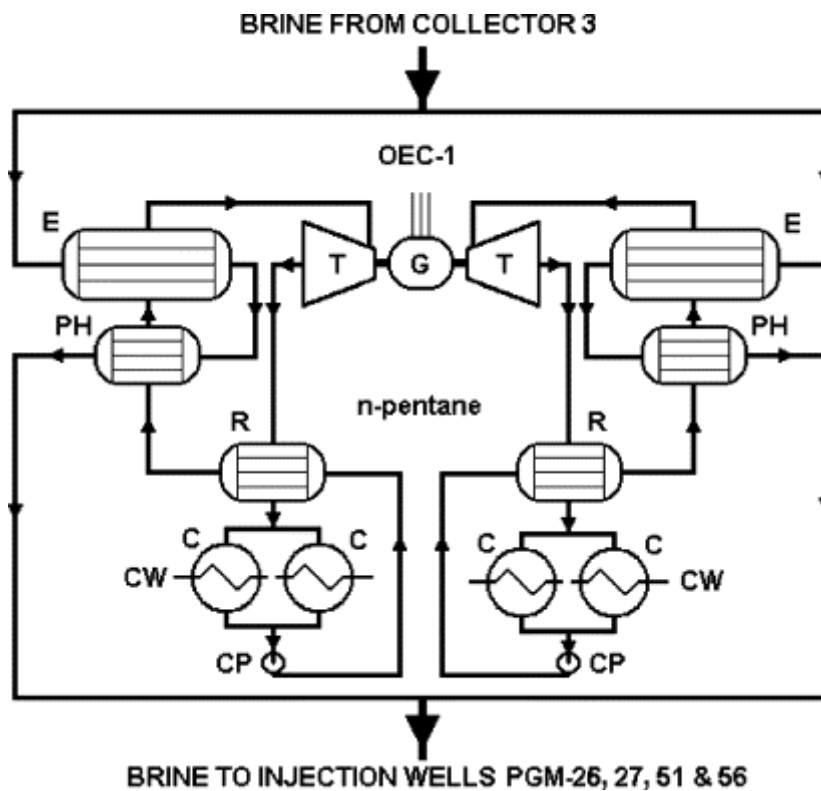


Figure 17. Simplified flow diagram for Unit 5 OEC-1. (E) Evaporator; (PH) preheater; (R) recuperator; (C) condenser; (CP) condensate pump; (CW) cooling water; (T) turbine; (G) generator.

After 2 years of operating life, the overall plant availability was 96.1%. The outlet brine temperature (upstream wells reinjection) is too low (120°C instead of 140°C) because of the oversizing of the condensers. Moreover, **clogging of the flowmeters** has been encountered (because of sand entrained in the brine) so bypass lines have been added at each of the brine headers. By periodically purging the headers, the operation of the meters improved, and coincidentally the potential for erosion in the tubes and connecting piping of the heat exchangers was likewise reduced.

Most of the geothermal wells of **Anatolia (Turkey)** have a temperature limit from 90 to 125°C. *Altun and Kilic (2020)* studied the **AFJET geothermal power plant** which started operating in 1994. The schematic diagrams of AFJET ORC power plant and the modified cycle with an Internal Heat Recovery exchanger are illustrated in Figure 18:

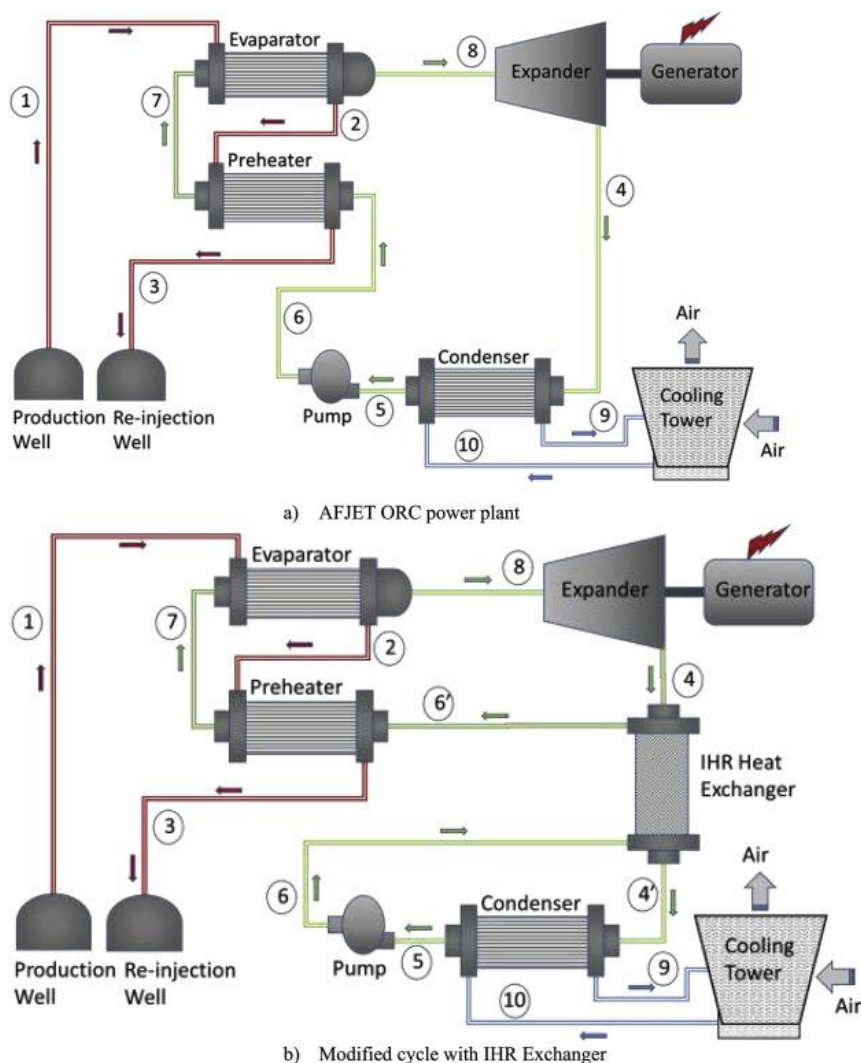


Figure 18. The schematic diagram of (a) AFJET ORC power plant, (b) Modified cycle with IHR Exchanger.

The ORC loop is composed of five components, which are an evaporator, a preheater, a condenser, an expander, and a pump. From point 5 to 6, the pump compresses the working fluid (**R-134a**) from the condensation pressure (537.5 kPa – 5.4bars) to the maximum pressure of the cycle (2503 kPa – 25bars).

The geothermal fluid is extracted at 121°C (well-head temperature) and 240 kPa with 81 kg/s flow rate. The geothermal fluid leaves the evaporator at 79.0°C and enters the preheater at state point 2. After most of the

energy of the geo-fluid is transferred to the working fluid which circulates in the ORC loop, geo-fluid is sent back to the re-injection well (State Point 3) at 54.8°C. The condenser is a **water-cooled condenser**.

Yildirim and Ozgener (2012) studied Aydın–Salavatli geothermal field’s features and the working principles of the two power plants (DORA 1 and DORA 2). Regarding DORA 1, the gross amount of power (full power) is 7.3 MW and its explicit power is 6.5 MW. Dora 1’s annual production capacity of electricity is 55,000,000 kWh. Figure 19 illustrates the DORA 1 central scheme:

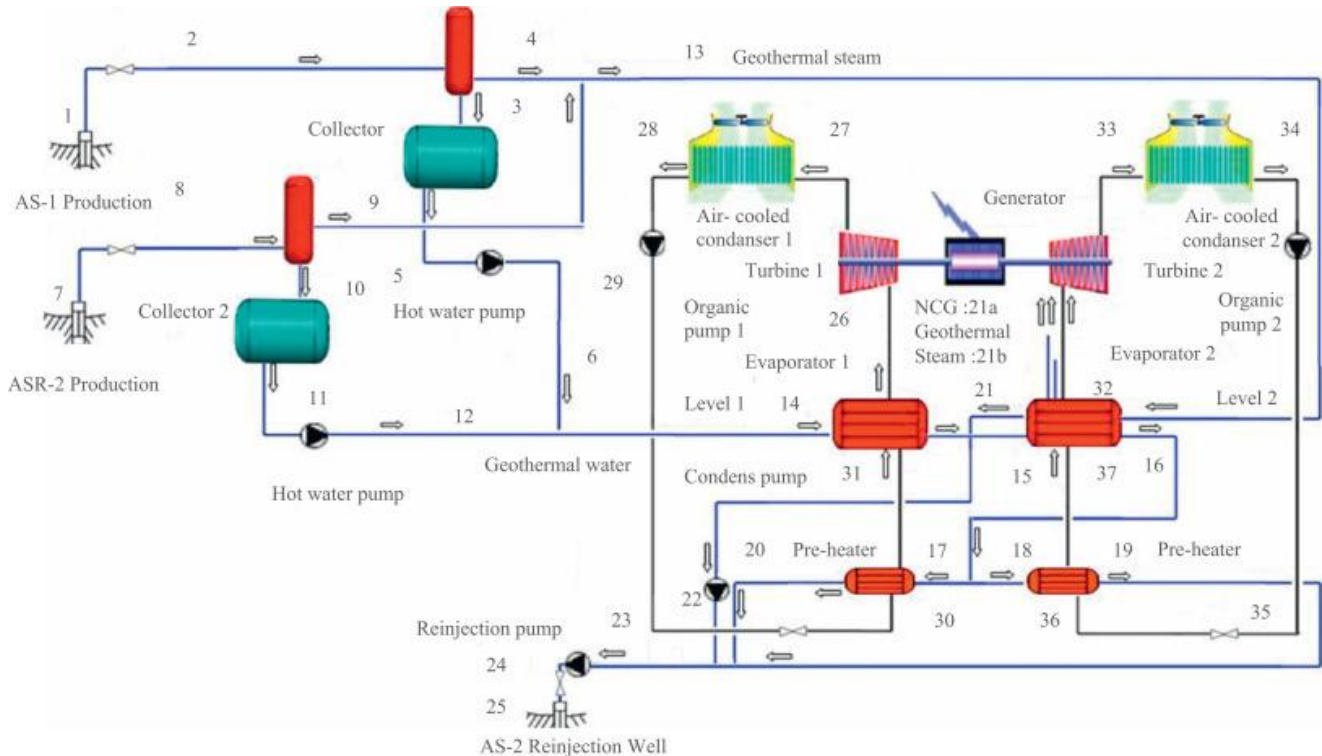


Figure 19. The schematic diagram of DORA I power plant.

The geothermal brine is 164°C and between 692 and 1170 kPa. The working fluid is **n-pentane**. The operating conditions in the evaporators are 137.6°C, 1200 kPa and 54.55 kg/s (evaporator 1) and 111.4°C, 750 kPa and 63.96 kg/s (evaporator 2). The pressure is reduced to 80 kPa (75.4°C) and 110 kPa (68°C) in Turbine 1 and Turbine 2, respectively. A temperature of around 35°C is reached downstream from the air-cooled condensers. Opened in May 2009, DORA 2’s gross power plant (installed capacity) is 11.2 MW and its absolute power plant is 9.8 MW. Annual production capacity of electricity is 85,000,000 kWh. The geothermal brine exits the wells at 176°C, 1600 kPa and around 115 kg/s.

N-pentane conditions in evaporator 1 are 136°C, 1149 kPa, 116.61 kg/s. It leaves turbine 1 at 81.3°C, 177 kPa and enters the air-cooled condenser. N-pentane is cooled to 40.4°C and then enters the Organic Pump 1. N-pentane conditions at the outlet of the organic Pump 1 are 41.5°C, 1070 kPa. Pre-heater 1 heats n-pentane up to 89.2°C upstream from the evaporator 1.

After flowing through the heat exchangers, the geothermal brine is reinjected in the wells at 83°C. The net power output from the Rankine cycle is 10.1 MW. It is further estimated based on the plant data that approximately 5.6% of the net power produced in the cycle is consumed parasitically by the plant unit, which corresponds to 623 kW. Parasitic power includes brine production pumps, cooling tower fans and other auxiliaries. Subtracting the parasitic power from the net power generated in the cycle, the net power output becomes 9.5 MW. The energy efficiency of the plant is calculated to be 10.7% (*Ganjehsarabi et al., 2012*).

Keçebas and Gökgedik (2015) cite the **Bereket GPP** (geothermal power plant). This is a two-level and binary power plant (Figure 20) that uses water for cooling and has a net electricity production capacity of 6.35 MW in the city of **Denizli, Turkey**. The plant was designed to operate using 145°C geothermal fluid separated at the flash plant, and the temperature of the fluid at the outlet of the binary plant is approximately 75°C. The working fluid is *n*-pentane.

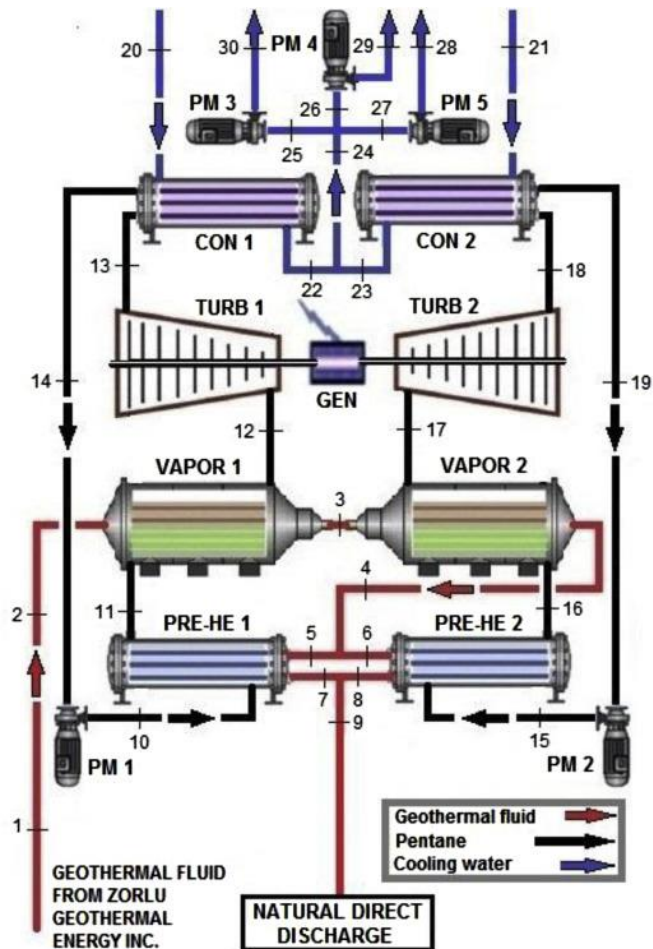


Figure 20. A schematic diagram of the Bereket GPP.

Guzovic et al. (2012) performed thermodynamic calculations based on the case study of the geothermal power plant of **Lunjkovec-Kutnjak (Croatia)**. The geothermal brine temperature is 140°C, the pressure is 6 bar, and the flow is 53 l/s for a natural outflow or 70 l/s with a submerged booster pump. The cooled geothermal fluid temperature is 80°C.

Thermodynamic calculations have been made with an **air-cooled condenser** assuming the average annual air temperature is 15°C. The working fluid is **isopentane**. For the medium-temperature geothermal resources, the following properties are preferable: low specific volumes, high efficiency (net power), moderate pressures in the heat exchangers, low cost, low toxicity, low ODP (ozone depletion potential), low GWP (global warming potential) and a low pinch-point temperature.

The authors compared the thermal efficiency of an ORC and a Kalina cycle and showed that for a medium-temperature geothermal source, the ORC is more appropriate (14.1 vs. 10.6%). This may be due to the relatively high temperature of the cold source (air temperature at 15°C) which is more unfavourable to the Kalina cycle.

Abisa (2002) describes the **Svartsengi geothermal power plant** located in Iceland. It is a high-temperature source with a reservoir temperature around 240°C. The Svartsengi Power Plant has five main power stations including Plant IV that was commissioned in 1989-1992 and produces only electricity with seven Ormat organic

turbines, 1.2 MWe each. The hot source is the exhaust steam from plant III (103°C). The working fluid is **isopentane**.

Four of the Ormat units are **air-cooled** and the other three are **water-cooled**. The working fluid is heated to 95°C in the boiler by the steam. The boiler is of the **shell and tube** type, which allows for an indirect heat exchanging system. The vaporised isopentane gas leaves the boiler and passes to the separator. The separator pressure is 6.2 bars.

Putera et al. (2019) selected the **Wayang Windu geothermal plant in West Java** to study the selection of the working fluid, the optimisation of the system performance, and the financial analysis. The fluids considered include **n-Pentane, Isopentane, and R245fa**, which are some of the most popular fluids in binary power plants. The average ambient temperature is 25.5°C at Pangalengan (West Java). The waste brine characteristics are 180.7°C, 1.02 MPa, 48 kg/s and a silica content of 853 mg/L.

The waste brine comes from the flash separation and is more concentrated with silica. Generally, in lower temperatures, the solubility of silica in geothermal fluids is also lower. Therefore, one of the most important design parameters in a binary power system is the **minimum temperature of brine utilisation to avoid scaling** issues. The authors give some design rules to evaluate this temperature.

An **air-cooled condenser** is considered for the thermodynamic model. The suggested minimum temperature difference between the working fluid and air was 10°C. There is no set of standard rules to specify the working parameters of a binary system. However, it is usually recommended to set the highest temperature of the working fluid in the cycle at 15°C below its critical point. Additionally, the highest pressure for the working fluid should not exceed 30 bar while considering the equipment compression capacity and the cost of the system. Near the critical point, the system can be unstable because large pressure changes may occur even with small temperature changes. Therefore, as the starting point, the limit for the inlet turbine temperature in this study was set 20°C below the geothermal brine temperature.

The most economically profitable working fluid in this work was n-pentane, obtained with the specific area optimisation approach.

Budisulistyo and Krumdieck (2015) performed thermo-economic evaluations of ORC for geothermal power plant in New-Zealand. The analysis used a typical geothermal resource in New Zealand with brine temperature of 173°C, pressure of 9 bar and flow rate of 8 kg/s.

The working fluids considered in this feasibility study are **R245fa, n-pentane and R134a** as these are most commonly used in the commercial ORC units. All the designs use **water-cooled condensers**. The recuperative and regenerative cycles using n-pentane have the smallest heat transfer area requirement, but the investment ratio is reduced due to higher condenser prices. For example the investment ratio drops from 0.942 to 0.636 for the two stage n-pentane standard cycle, and from 0.865 to 0.562 for two stage n-pentane regenerative cycle when air cooled condensers are used. These results assume that the specific power consumed by fans of the air-cooled condenser is 0.15 kW per kg/s of air flow.

Zarrouk et al. (2014) describe the two power generating units that were installed at the Wairakei power-station, New-Zealand, in 2005. These units have been used to utilise heat from brine destined for reinjection. They operate on an “Organic Rankine Cycle”, in which a volatile hydrocarbon (**pentane** C₅H₁₂ in this case) is employed as the motive fluid. The binary power plants at Wairakei use a series of **shell and tube heat exchangers** in order to extract heat from the geothermal brine and evaporate/superheat the motive fluid. Table 18 gives some detailed data.

Table 18. Summary of fluid states in the Wairakei binary plants, as per design.

Brine entering	Pressure (bar)	Temperature (°C)	Mass flow (tonne/h)
Level 1 Vaporizer	5.9	127	1400
Level 2 Vaporizer		111	1400
Level 1 Pre-heater		101	700
Level 2 Pre-heater		101	700
Brine Return	3.2	87	1400
Pentane in Level 1 circuit entering			
Pre-heater		45	315
Vaporizer		95	315
Turbine	8.8	109	315
Air cooled condenser	1.2	33	315
Recuperator		29	315
Pentane in Level 2 circuit entering			
Pre-heater		24	222
Vaporizer		97	222
Turbine	6.9	97	222
Air cooled condenser	1.0	28	222
Recuperator		24	222

At the mean air temperature at Wairakei of 12°C, the power plants are designed to produce a net power output of 7285 kW each from 2800 tonne/h (1400 tonne/h per machine) of brine that is previously rejected at about 131°C. The brine is reinjected at about 87°C after going through the binary plant.

The scaling is cleaned by hydroblasting every six months, but this comes at high cost and several days of lost generation time.

Tomarov et al. (2010) and *Tomarov and Shipkov (2017)* describe the 2.5 MW binary cycle power unit in the Pauzhetskaya GeoPP, Kamchatka. The heat source is a waste liquid phase of the Pauzhetskaya GeoPP at a temperature of 120°C. The organic refrigerant compound **R-134a** was selected as the working fluid. The **evaporator-superheater**, which is made as a **shell-and-tube** apparatus, houses three heat transfer surfaces in a common shell: an economiser, an evaporator, and a vapor superheater. The condenser is designed as a **shell-and-tube heat exchanger** using cooling water at a temperature of 8°C (23°C at the outlet of the condenser with a cooling flowrate of 1500m³/h).

Kahraman et al. (2019) performed thermodynamic and thermo-economic analysis for an operating **air-cooled** binary type GPP. The plant is located at **Aydin Germencik (Sinem GPP)**. The heat exchangers are **shell and tube HX**. Table 19 gives some plant specifications.

Table 19. System description of the geothermal power plant.

Parameter	Value	Unit
Gross power	21.25	MW _e
Net power	18.50	MW _e
Cooling system	Dry Air Cooling	–
Working fluid	n-pentane	–
Source temperature	168.2	°C
Sink temperature	17.5	°C
Brine reinjection temperature	78.5	°C

DiPippo (2016) describes several case studies. Among them are some binary power plants:

- In New-Zealand, besides Wairakei (*Zarrouk, 2014*), the power plant of **Ngatamariki** (New-Zealand) also operates a binary cycle. It was the largest binary power station in 2014 with 82 MW net produced from four identical ORC. The working fluid is **pentane**. Condensers are **air-cooled** heat exchangers (with each

Date: 31 March 2020

25/20.5 MW unit). The brine wellhead temperature is 193°C. Pre-heaters and evaporators seem to be **shell-and-tube** heat exchangers.

- In San Salvador, the **Berlín power plant** is made of three single-flash units and a 8 MW bottoming binary cycle. The brine temperature is 180°C and the working fluid is **isopentane**. The condensers are **shell-and-tube heat exchangers** with inlet and outlet water temperatures of respectively 28 and 38°C. An experiment was conducted in 2014 with solar collectors to raise the temperature of the waste brine from the bottoming binary cycle. The objective is to **alleviate silica scaling**.
- In Guatemala, the **Zunil power plant and the Amatitlán power plant** operates ORC to generate respectively 25 MWnet and 20 MW. Condensers are **air-cooled** type. The brine temperature is around 180°C.
- The **Magmamax** binary power plant is located in California, USA. The construction started in 1979 and the net power is 11 MW. Evaporators are **shell-and-tube** heat exchangers. However, an **unusual configuration** was adopted because of specific operating conditions (pressure of working fluid, 41 bar, higher than pressure of brine); the brine was placed on the shell side and the working fluid (**isobutane and propane**) on the tube side. There was no baffle in the shell and a counter-flow configuration was used. The recuperator (see figure 21) was a **single tube pass** heat exchanger.

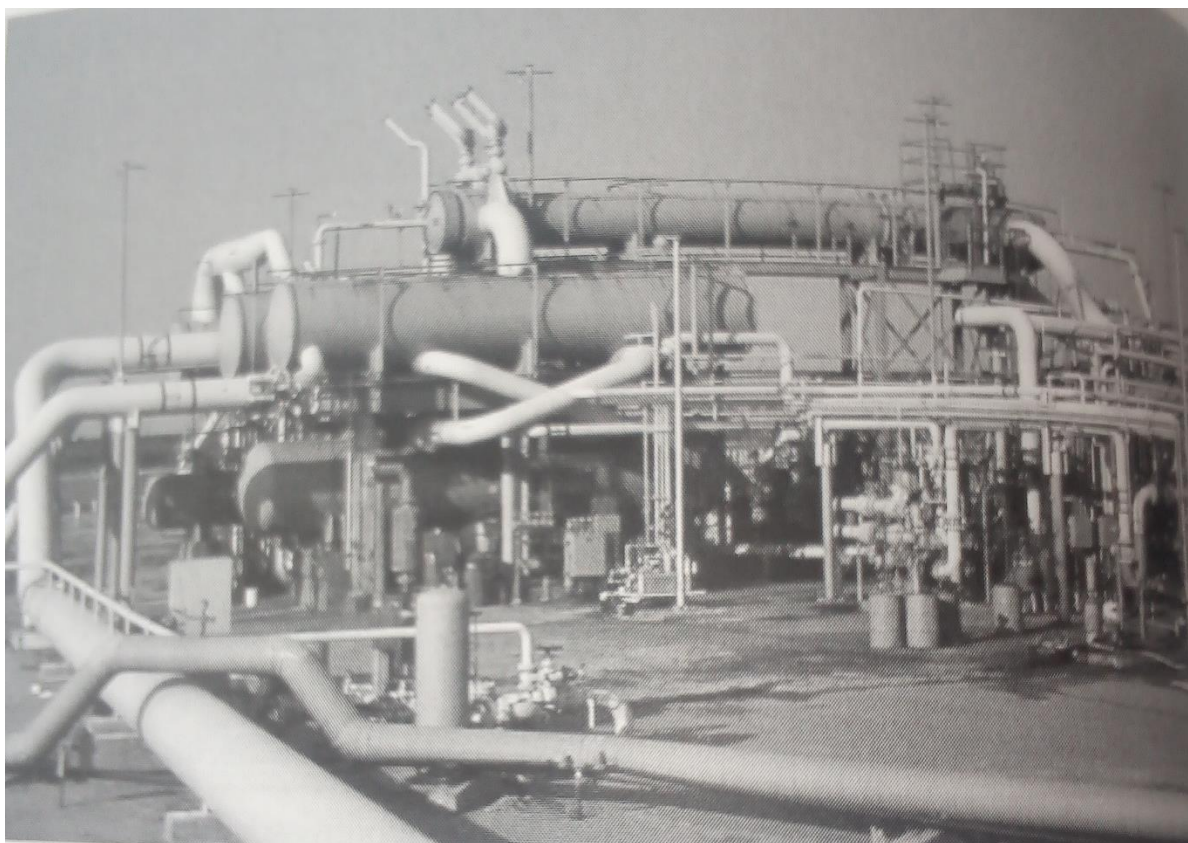


Figure 21: Condensers and recuperator (upper vessel) at Magmamax plant.

Because of high daytime temperatures (50°C) but clear nights, a phased cooling system with daytime storage and nighttime cooling via spray bonds was used. However because of **corrosion and mechanical damage** (excessive vibrations) in the heat exchangers, the power plants only operated for two years. The 0.9-mm thick **carbon steel tubes** were undergoing corrosion at rates of between 0.13 and 0.6 mm/year. The reconfigured plant involve **new shell-and-tube heat exchangers** with brine on the tube side and hydrocarbons on the shell side. A pressure-letdown valve was inserted to lower the isobutane pressure. It was commissioned in 1982. The brine inlet temperature is 176°C.

4.3.3 Heat exchangers

4.3.3.1 Overview

Various heat exchangers are involved in ORC systems. First of all, the brine transfers its heat to the working fluid through the evaporator. Then the working fluid condenses in either a water-cooled condenser or an air-cooled condenser. Finally, additional one-phase heat exchangers allow heat recuperation to pre-heat the working fluid upstream from the evaporator or to recover heat from the working fluid (desuperheating) upstream from the condenser to preheat the condensate. *DiPippo (2016)* gives some approximate values for the global heat transfer coefficients of heat exchangers in an ORC unit (see Table 20).

Table 20: Approximate values for overall heat transfer coefficient in ORC heat exchangers (DiPippo, 2016).

Fluids	Overall heat transfer coeff. (W/m ² .K)
Propane or butane (condensing) - Water	700 – 765
Refrigerant (condensing) - Water	450 – 850
Refrigerant (evaporating) - Brine	170 – 850
Steam – Gases	30 – 285
Steam – Water	1000 – 3400
Steam (condensing) – Water	1000 – 6000
Water - Air	25 – 50
Water - Brine	570 – 1135
Water - Water	1020 - 1140

4.3.3.2 Evaporators

Shell & Tube (S&T) heat exchangers:

Most evaporators described in the literature are **Shell & Tube (S&T)** heat exchangers. Among the different types of heat exchangers, shell and tube heat exchangers are preferred for space heating, power production, and chemical processing applications. The main advantages of this heat exchanger type over other types can be listed as follows:

- There is substantial flexibility regarding their materials to accommodate corrosion and other concerns;
- They can be used in systems with higher operating temperatures and pressures;
- Tube leaks are easily located and plugged since pressure test is comparatively easy.

However, this kind of heat exchanger requires more space, and cleaning and maintenance are difficult since a tube requires sufficient amount of clearance at one end to remove the tube nest (*Erdogan et al., 2017*). In general, the evaporator/superheater is a **horizontal cylinder or a kettle-type boiler** with an optional superheating section. **Brine flows in the tubes and the working fluid is on the shell side** (*DiPippo, 2016*). *Welzl et al. (2020)* use a S&T heat exchanger with boiling in the shell side and copper tubes in a 1 kW ORC test rig with a 1kW (saturation temperature from 85 to 105°C). The working fluids are R245fa (high GWP) and R1233zd(E). *Astolfi et al. (2014)* performed thermodynamic calculations based on a S&T evaporator arranged either in a **once-through configuration** in supercritical cycles or as a **kettle reboiler** evaporator in subcritical cycles. The Husavik geothermal power plant (*Mlcak et al., 2002*) operates a Kalina cycle. The evaporator is a shell-and-tube exchanger utilising **low-fin carbon steel** tubes.

Schochet (1997) describes ORMAT geothermal power plants. For the case of high temperature resources (>190°C), the “wetter” steam (after the hotter, drier steam flew through a steam turbine) is condensed in the tubes of a **shell and tube heat exchanger** for the vaporisation of the organic fluid (ORC).

The vaporiser of the Svartsengi geothermal power plant (*Abisa, 2002*) is a **shell and tube heat exchanger**. Isopentane flows in the shell while steam is in the tubes. The separator is welded on the top of it to remove droplets of liquid, and fitted with a safety valve. Normal operating parameters are:

- Heat source inlet temperature 103°C.
- Heat source outlet temperature 95°C.
- Flow rate 18720 kg/hr.

The evaporator-superheater of the binary cycle unit at the Pauzhet geothermal power station uses the steam–water mixture arriving from the production wells at the Pauzhet geothermal field with a temperature of 120°C (*Tomarov and Shipkov, 2017; Tomarov et al., 2014*). This **shell and tube heat exchanger** combines three heat exchangers—economiser, evaporator, and vapor superheater—in one casing. The heating source flows in a **five-pass tube bundle** (one-pass superheater, two-pass evaporator, two-pass economiser). The heat transfer surface evaporating part is located above the economiser. The economiser is closed by thin walled sheets in order to organise eight pass counter and crosscurrent flow. The economiser surface is arranged with 949 tubes. Superheated vapor generated in the vapor superheater enters via nine pipes with a 150 mm nominal diameter into the vapor header, vapor from which is supplied to the turbine inlet (see Figure 22). The geothermal heat source is quite corrosive (chlorides from 200 to 1170 mg/L and total mineralisation equal to 1.3 g/L). The evaporator type vapor superheater tube system is made of Grade 10Kh17N13M2T **stainless steel**, and the 40 mm thick tube sheets are made of Grade 12Kh18N10T **stainless steel**. The evaporator type vapor superheater shell (barrel) is made of Grade 08Kh18N10T **stainless steel**. The pipelines are made of Grade 20 **carbon steel**.



Figure 22: Evaporator type vapor superheater used in the Pauzhet GeoPS binary power unit with a cluster of feed pumps.

The evaporators of the Miravalles geothermal site (*Moya and DiPippo, 2007*) are **horizontal shell-and-tube** heat exchangers similar to the preheaters, but larger (Figure 23). There are two per module, each having a total of 1744 tubes, 19.45 mm in diameter, 10.86 m long and fabricated from 316L **stainless steel**, within a 14.2 m long, 1.42 m diameter shell. The tube bundle is fixed.

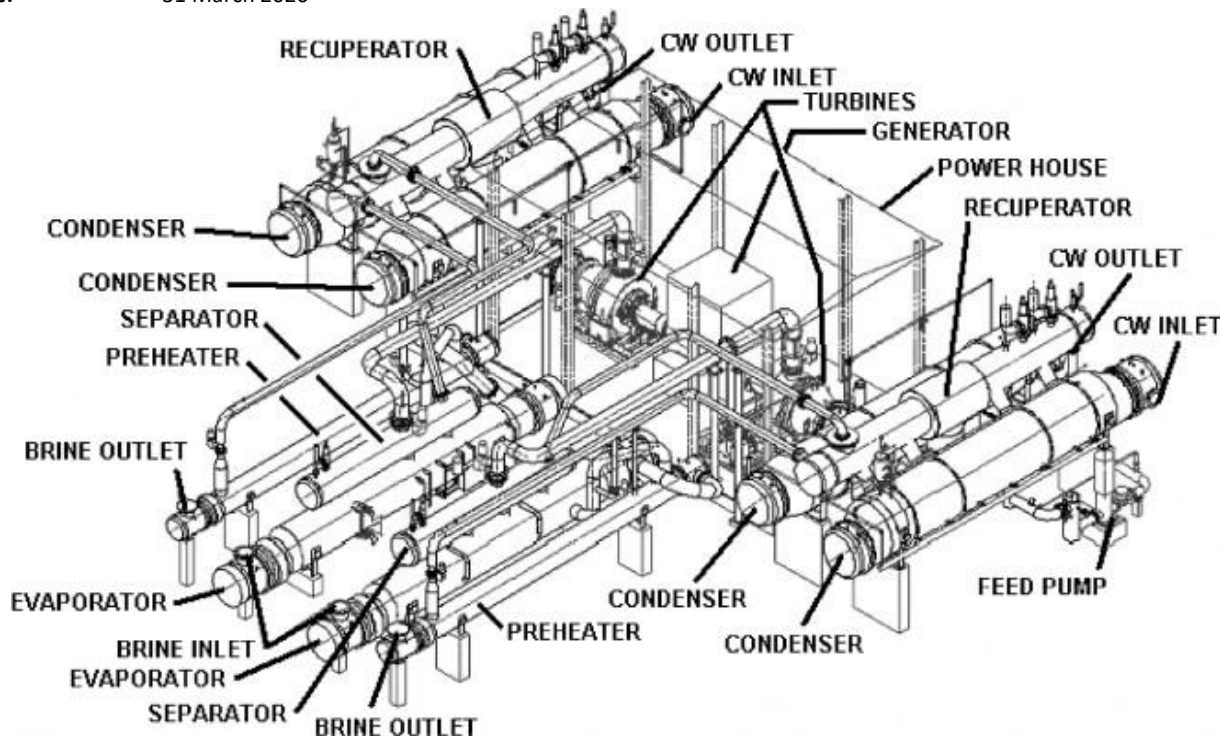


Figure 23. Unit 5 energy conversion module: one of two identical Ormat® Energy Converters (OECs).

Pasek et al. (2011) detailed components of the plant located in Lahendong, North Sulawesi (Indonesia). The evaporator is a **shell & tube heat exchanger**. The material for the shell is **carbon steel ASTM a516-60**, because the shell will be passed with working fluid. The tubes used **duplex stainless steel SAF 2205 (ASTM 789)**, because the tubes will be passed with brine which has a high chloride content and low pH (sour). Duplex stainless steel will resist uniform corrosion and pitting (localised corrosion). The evaporator will be a **kettle type (AKT)** according to TEMA standards. The input process and design parameters required for the design of the evaporator are provided in Tables 21 and 22:

Table 21. Input layout when design evaporator.

Process conditions					
Flow rate	Hot tube	108.38	Cold shell	34.49	kg/s
Inlet/outlet Y	0	0	0	1	Weight fraction vapor
Inlet/outlet T	158.9	143.8			°C
Inlet P/allow dP	600	50	1530	50	kPa/kPa
Fouling resistance	0.0003		0.0002		m ² K/W
Shell geometry					
TEMA type	AKT				
Inside diameter	1550	mm			
Orientation	Horizontal				
Hot fluid	Tubeside				
Tube geometry					
Type	Plain		Wall thickness	1.651	mm
Length	8.534	m	Layout angle	45	°
Tube OD	25.4	mm	Tubepasses	2	
Pitch	32	mm			

Table 22. Output result from evaporator thermal design.

Process conditions		Cold shellside i-Pentane		Hot tubeside Brine	
Fluid name					
Flow rate	(kg/s)		34.4943		108.376
Inlet/outlet Y	(Wt. frac vap.)	0	1	0	0
Inlet/outlet T	(°C)	138.8	138.9	158.9	143.8
Inlet P/Avg	(kPa)	1530.02	1528.38	600	598
dP/Allow.	(kPa)	3.287	50	4.01	50
Fouling	(m ² K/W)		0.0002		0.0003
Exchanger performance					
Shell h	(W/m ² K)	2856.9	Actual U	(W/m ² K)	783.5
Tube h	(W/m ² K)	3974.37	Required U	(W/m ² K)	685.98
Hot regime	(-)	Sens. liquid	Duty	(MW)	7.274
Cold regime	(-)	Flow	Area	(m ²)	983.927
EMTD	(°C)	10.8	Overdesign	(%)	14.22
Shell geometry			Baffle geometry		
TEMA type	(-)	AKT	Baffle type	(-)	Support
Shell ID	(mm)	1550	Baffle cut	(Pct Dia.)	
Series	(-)	1	Baffle orientation	(-)	
Parallel	(-)	1	Central spacing	(mm)	1673.07
Orientation	(°)	0	Crosspasses	(-)	1
Tube geometry			Nozzles		
Tube type	(-)	Plain	Shell inlet	(mm)	205.004
Tube OD	(mm)	25.4	Shell outlet	(mm)	307.087
Length	(m)	8.534	Inlet height	(mm)	59.545
Pitch ratio	(-)	1.2598	Outlet height	(mm)	965.865
Layout	(°)	45	Tube inlet	(mm)	307.087
Tubecount	(-)	1474	Tube outlet	(mm)	307.087
Tube Pass	(-)	2			
Thermal resistance, %		Velocities, m/s		Flow fractions	
Shell	27.43	Shell side	0.17	A	0
Tube	22.66	Tubeside	0.43	B	1
Fouling	41.52	Crossflow	0.11	C	0
Metal	8.397	Window	0	E	0
				F	0

The binary power plants at Wairakei (Table 23) use a series of **shell and tube heat exchangers** in order to extract heat from the geothermal brine and evaporate/superheat the motive fluid (Zarrouk *et al.*, 2014). Geothermal fluid passes through the tube-side and the pentane passes through the shell-side of the heat exchanger. All the heat exchangers in the binary plants contain heat exchanger tubes with internal diameters of 22 mm and of 11.6 m in length. The first heat exchanger in the series is arranged in a **three pass configuration**; meaning that the brine flowing through it travels the length of the shell three times, turning back at the end of the shell, before exiting. The brine in the other heat exchangers, and the two pre-heaters, flows through **two passes** before leaving the heat exchanger.

Table 23. Summary of fluid states in the Wairakei binary plants, as per design.

Brine entering	Pressure (bar)	Temperature (°C)	Mass flow (tonne/h)
Level 1 Vaporizer	5.9	127	1400
Level 2 Vaporizer		111	1400
Level 1 Pre-heater		101	700
Level 2 Pre-heater		101	700
Brine Return	3.2	87	1400
Pentane in Level 1 circuit entering			
Pre-heater		45	315
Vaporizer		95	315
Turbine	8.8	109	315
Air cooled condenser	1.2	33	315
Recuperator		29	315
Pentane in Level 2 circuit entering			
Pre-heater		24	222
Vaporizer		97	222
Turbine	6.9	97	222
Air cooled condenser	1.0	28	222
Recuperator		24	222

Plate-type heat exchangers:

Kose (2007) and *Arslan and Kose (2010)* report the State of the art of geothermal energy in Turkey. At the wellhead of the Simav geothermal system, the geothermal fluid has a temperature of 147°C and a return temperature of 40°C. The scaling and corrosion problems have been solved by an inhibitor (5 g/m³), epoxy fiberglass pipe, 316L **stainless steel plate-type heat exchanger** and partially by CO₂ and H₂S separation.

Hettiarachchi et al., 2007 considered flat **plate-type** heat exchangers (shell-and-plate heat exchanger) in the optimisation study for both evaporator and condenser. Plate-type heat exchangers are preferred in this analysis due to their compactness and high heat transfer coefficients which result in less heat transfer area than would be needed for the same duty using shell and tube heat exchanger. The HX material is titanium.

Imran et al. (2016) modelled a complete ORC system; the authors developed an independent model of each component: evaporator, condenser, expander and the working fluid pump. The evaporator model has been constructed on the basis of a **plate-type evaporator** (chevron plate profile, see Figure 24 and Table 24).

Table 24. Geometrical parameters of plate heat exchanger.

Parameter	Value
Effective Width (W_e)	0.650 m
Corrugated Pitch (P_{co})	0.0085 m
Plate Spacing (b)	0.0025 m
Plate Thickness (t)	0.0005 m
Chevron Angel (β)	60 Degree

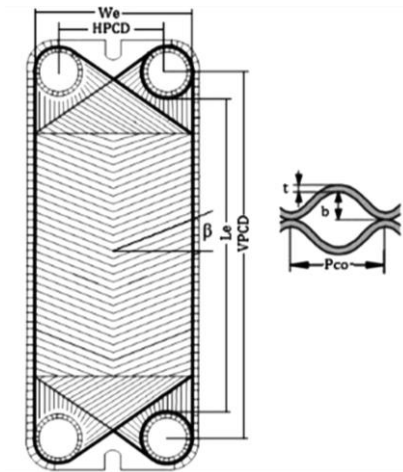


Figure 24. Geometrical profile of plate heat exchanger.

Muhammad *et al.* (2015) present an experimental investigation of a small scale (1 kW range) organic Rankine cycle system for net electrical power output ability, using low-grade waste heat from steam (low pressure steam as heat source which is an abundant industrial waste heat source). The working fluid is R245fa. The heat exchangers are **brazed plate-type HX**. The heat exchangers have 60 plates, with total heat transfer area of 6.5 m². Overall heat transfer coefficient was identified as 756 W/m²/K. Maximum pressure drop is less than 30 kPa on the working fluid side.

4.3.3.3 Recuperators/preheaters

Preheaters are liquid/liquid heat exchanger either horizontal cylinder **shell-and-tube type** with brine on tube side and working fluid on shell side or vertical **corrugated plate-type** heat exchanger (DiPippo, 2016).

The Husavik geothermal power plant operates a Kalina cycle (Mlcak *et al.*, 2002). The high temperature recuperator is a **carbon steel shell-and-tube exchanger**. The low temperature recuperator is a **welded plate exchanger**. The plates are **stainless steel** surrounded by a **carbon steel housing**.

In the Miravalles geothermal power plant (Moya and DiPippo, 2007), the ORC unit, illustrated in Figure 23 involves:

- **Horizontal shell-and-tube** pre-heaters, each having a total of 743 tubes, 19.45 mm in diameter, 11.48 m long, and fabricated from 316 L **stainless steel**, with a welded tube-to-tube sheet connection, within a 13.87 m long, 0.78 m diameter **shell made of carbon steel**. The brine flows through the tubes and the pentane flows within the shell. The tube bundle is fixed.
- Two horizontal, **shell-and-tube recuperators** per module. The hot turbine exhaust passes over tubes in which flows the pentane discharged from the feed pumps. In each recuperator, there are a total of 544 tubes, 25.7 mm in diameter and 9.80 m long; the vessel is 1.625 m in diameter and is 11.72 m long.

Pasek *et al.* (2011) detailed components of the plant located in Lahendong, North Sulawesi (Indonesia). The preheater is a **shell & tube heat exchanger**. The material for the **shell is carbon steel** ASTM a516-60, because the shell will be passed with working fluid. The tubes used duplex stainless steel SAF 2205 (ASTM 789), because the tubes will be passed with brine which has a high chloride content and low pH (sour). **Duplex stainless steel** will resist uniform corrosion and pitting (localised corrosion). The preheater will be a **two pass shell type** (AFT) according to TEMA standards. The input process and design parameters required for the design of preheater are given in Tables 25 and 26:

Table 25. Input layout when design preheater.

Process conditions					
Flow rate	Hot tube	108.38	Cold shell	34.49	kg/s
Inlet/outlet Y	0	0	0	0	Weight fraction vapor
Inlet/outlet T	143.79	125	41.19	138.8	°C
Inlet P/allow dP	600	50	1574.05	50	kPa/kPa
Fouling resistance	0.0003		0.0002		m ² K/W
Shell geometry			Baffle geometry		
TEMA type	AFT		Type	Single segmental	
Inside Diameter	1420	mm	Cut	25	%
Orientation	Horizontal		Spacing	600	mm
Hot fluid	Tubeside				
Tube geometry					
Type	Plain		Wall thickness	1.651	mm
Length	8.534	m	Layout angle	45	°
Tube OD	25.4	mm	Tubeypasses	2	
Pitch	32	mm			

Table 26. Output result from preheater thermal design.

Process conditions		Cold shellside		Hot tubeside	
Fluid name		i-Pentane		Brine	
Flow rate	(kg/s)		34.4943		108.379
Inlet/outlet Y	(Wt. frac vap.)	0	1	0	0
Inlet/outlet T	(°C)	41.19	138.8	143.8	125
Inlet P/Avg	(kPa)	1574.07	1564.34	600	597.65
dP/Allow.	(kPa)	19.469	50	4.725	50
Fouling	(m ² K/W)		0.0002		0.0003
Exchanger performance :					
Shell h	(W/m ² K)	1306.09	Actual U	(W/m ² K)	595.48
Tube h	(W/m ² K)	4415.01	Required U	(W/m ² K)	514.19
Hot regime	(-)	Sens. Liquid	Duty	(MW)	9.155
Cold regime	(-)	Sens. Liquid	Area	(m ²)	822.183
EMTD	(°C)	21.7	Overdesign	(%)	15.81
Shell geometry			Baffle geometry		
TEMA type	(-)	AFT	Baffle type	(-)	Single-Seg.
Shell ID	(mm)	1420	Baffle cut	(Pct Dia.)	25
Series	(-)	1	Baffle orientation	(-)	Parallel
Parallel	(-)	1	Central spacing	(mm)	600
Orientation	(°)	0	Crosspasses	(-)	13
Tube geometry			Nozzles		
Tube type	(-)	Plain	Shell inlet	(mm)	205.004
Tube OD	(mm)	25.4	Shell outlet	(mm)	205.004
Length	(m)	8.534	Inlet height	(mm)	64.135
Pitch ratio	(-)	1.2598	Outlet height	(mm)	64.135
Layout	(°)	45	Tube inlet	(mm)	307.087
Tube count	(-)	1230	Tube outlet	(mm)	307.087
Tube Pass	(-)	2			
Thermal resistance, %		Velocities, m/s		Flow fractions	
Shell	45.59	Shell side	0.43	A	0.092
Tube	15.5	Tubeside	0.5	B	0.639
Fouling	32.45	Crossflow	0.49	C	0.124
Metal	6.46	Window	0.68	E	0.144
				F	0

4.3.3.4 Condensers

The power consumption of the cooling system of the ORC may reach up to **30% of the turbine output** (Alimonti et al., 2019). For binary geothermal power plants using air as the cooling medium, the condenser temperature varies as the ambient air temperature fluctuates throughout the year and even throughout the day. As a result, the power output decreases by up to 50% from winter to summer. Consequently, the exergy destruction rates and percentages at various sites change, this effect being most noticeable in the condenser (Kanoglu and Bolatturk, 2008).

When surface water (once-through systems), wet-type cooling towers, and dry-type cooling towers type cooling systems for geothermal binary plants are compared, cooling with **surface water provides the highest efficiency**

Date: 31 March 2020

while requiring the highest cold water supply. In terms of costs, **dry cooling is the most expensive** cooling option (Kanoglu and Bolatturk, 2008; Budisulistyo and Krumdieck, 2015).

Mendrinós et al. (2006) investigated several cooling systems: (i) Surface water (once-through systems), (ii) Wet type cooling towers and (iii) Dry type cooling towers.

For surface water systems, the cooling fluid is water, which is transported to the power plant through pipes from a river, a lake or the sea. Its main advantage is that it can yield the lowest possible condensing temperature, and hence the maximum conversion efficiency. Binary plants normally use horizontal **double pass shell-and-tube heat exchangers** as surface condensers, with the cooling water flowing inside the tubes and the steam and condensate in cross flow within the shell. Although not a standard practice, use of **plate heat exchangers** instead, may be a tempting option due to their compact size, their mass production (lower cost), ease of dismantling/reassembly, ease of cleaning, and their high overall heat transfer coefficient, typical values of which are 10-20 kW/m².

For flash plants, wet cooling towers are usually coupled with **direct contact condensers**, where the cooling water is sprayed and mixed with the steam condensate, and which are simpler in design and much more cost effective than surface condensers used in binary plants. For this reason, **direct contact condensers and wet type cooling towers are the standard technology in geothermal flash plants**. Exceptions are encountered in cases where large quantities of surface water are available locally, and in extremely cold climates in order to avoid frosting water droplets precipitating in the plant neighbourhood.

Due to the need for many times higher heat exchange surface and the large volume of air that has to be moved through them, **dry type cooling towers are the most expensive option**. A dry type cooling tower costs 5-10 times as much as a wet type one depending on the condensing temperature of the turbine. However, in cases of lack of water, strict local water use regulations, extremely low ambient temperatures during winter which cause water droplets from wet type cooling towers to freeze onto nearby vegetation, dry type cooling towers may be the only available option. **Most commercial geothermal binary power plants use air-cooled condensers** because of the issues of resourcing and pumping cooling water (Budisulistyo and Krumdieck, 2015).

Shell-and-tube heat exchangers:

Mendrinós et al. (2006) assessed the heat transfer coefficient of a simplified **shell-and-tube condenser** with correlations from the literature (laminar film condensation on horizontal tubes). The authors conclude that the surface area of a water-cooled condenser can be approximately 25 times less than an air-cooled one. The total heat transfer coefficient of a water-cooled condenser is ~5600 W/m²/K when the air-cooled condenser is only ~100 W/m²/K. Costs for air-cooled condensers should therefore be higher than water cooled ones. For conversion efficiencies of 6.96% and 6.78% respectively, heat exchange areas are 88 m² for the water-cooled condenser and 3160 m² (36 times larger) for the air-cooled heat condenser. However, dry air type cooling towers, despite adverse economics and energy efficiency, may be the only feasible option in cases of water scarcity, or **extreme climatic conditions**.

As well as the evaporators and recuperators, the condensers of the Miravalles geothermal unit (Moya and DiPippo, 2007) are **shell-and-tube heat exchangers**, four per module (see Figure 23). Cooling water flows through the tubes and condenses the pentane that passes through the shell. Each condenser has a total of 2750 tubes, 19.3 mm in diameter and 10.97 m long; the overall diameter of the vessel is 1.97 m and it is 13.5 m long.

The 2.5 MW binary cycle power unit in the Pauzhetskaya GeoPP, Kamchatka (Tomarov and Shipkov, 2017; Tomarov et al., 2014) is fed with a waste liquid phase of the Pauzhetskaya GeoPP at a temperature of 120°C. The organic refrigerant compound R-134a was selected as the working fluid. The condenser is essentially a **shell-and-tube heat exchanger** designed to maintain the condensation temperature equal to 22°C with the cooling water temperature equal to 8°C (Fig. 25). The condenser casing is a 7040 mm long cylindrical barrel with an inner diameter of 1900 mm and 20 mm thick wall (Figure 25). The condenser was manufactured in the smooth tube version has the following design features: (i) The condenser casing and tube sheets are under the pressure of saturated organic fluid vapor equal to 0.75 MPa. (ii) The condenser is installed with a 4° slope to the horizontal

Date: 31 March 2020

plane to reduce the influence of tube bundle flooding by condensate from the upper tubes, thus achieving more efficient heat transfer. The volume of working fluid is 15 m³. The condenser tubes (16 mm in diameter, with the 1.0 mm thick wall and 6600 mm long) were made of Grade 10Kh17N13M3T **stainless steel**, and the 40 mm thick tube sheets were made of Grade 12Kh18N10T **steel**.



Figure 25: Condenser of the binary turbine unit at the Pauzhet GeoPS.

Two types of condenser are used in the Svartsengi geothermal power plant (Abisa, 2002):

- Water cooler - horizontal **tube and shell type heat exchanger**;
- Air cooler - condenses the working fluid of four units of the power plant.

Plate-type heat exchangers:

In Husavik, Iceland, Kalina cycle (Mlcak et al., 2002), the condensers are **plate-type heat exchangers** with welded pairs on the ammonia-water process side to minimise leakage. Plates are **stainless steel**. There are two 50% capacity condensers arranged in parallel.

Muhammad et al. (2015) present an experimental investigation of a small scale (1 kW range) organic Rankine cycle system for net electrical power output ability, using low-grade waste heat from steam (low pressure steam as heat source which is an abundant industrial waste heat source). The working fluid is R245fa. The heat exchangers are **brazed plate-type HX**. Model BC-50 with 50 plates was provided as a suitable condenser. The heat exchanger has an area of 5.38 m². Pressure loss for the working fluid side is less than 10.6 kPa.

Hettiarachchi et al., 2007 considered flat plate-type heat exchangers (**shell-and-plate heat exchanger**) in the optimisation study for both evaporator and condenser. Plate-type heat exchangers are preferred in this analysis due to their compactness and high heat transfer coefficients which result in less heat transfer area than would be needed for the same duty using shell and tube heat exchanger. The HX material is **titanium**. The specifications are listed in Table 27.

Table 27. Specifications of the Organic Rankine Cycle considered

Working fluids	Ammonia, n-Pentane, HCFC-123, PF 5050
Gross power W_{Gross}	10 MWe
Condenser and evaporator	Shell and plate type [14,15] Heat transfer plate material is titanium $l = 1460$ mm, $w = 550$ mm, $t = 0.6$ mm, $\delta x = 5$ mm, $\delta y = 5$ mm
Geothermal water temperature T_{HWI}	70–90 °C
Geothermal water and cooling water pump efficiency η_{WP}	0.80
Working fluid pump efficiency η_{WFP}	0.75
Cooling water temperature T_{CWI}	30 °C
Turbine efficiency η_T	0.85
Generator efficiency η_G	0.96

The same kind of heat exchanger (Figure 26) is used for OTEC (Ocean Thermal Energy Conversion) systems (Nakaoka and Uehara, 1988a, 1988b). The authors characterised the performances (heat transfer coefficient and pressure drops) of **plate and shell heat exchangers**. The working fluid is Freon 22 for the condenser and Freon 22 and ammonia for the evaporator. The available temperature difference in such systems is small (15–23 °C) and the evaporator/condenser are major cost items (20–50%) of an OTEC plant. The plate type condenser heat exchange area is 40.7 m² (168 plates of 0.242 m² each) while the evaporator area is 21.95 m² (100 plates).

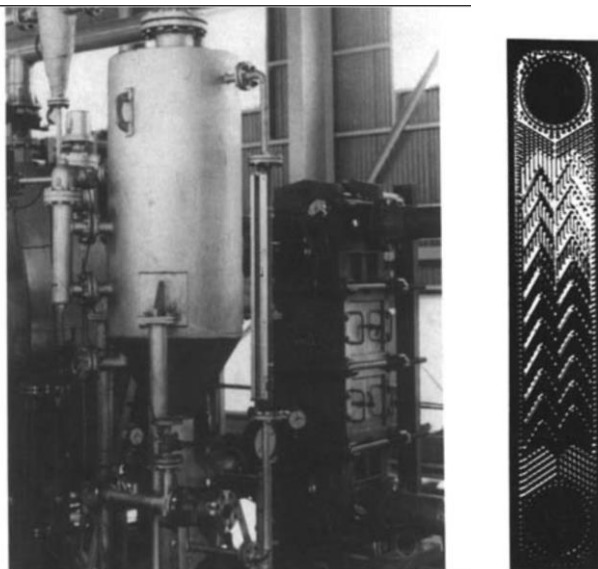


Figure 26: Shell-and-plate type evaporator (left side) and plate details (right side), Nakaoka and Uehara, 1988a, 1988b.

Chen et al. (2019) also implemented a 15 kW OTEC system with ORC including **plate heat exchangers** for both evaporator and condenser. The working fluid is ammonia.

Alimonti et al. (2019) studied a Well Bore heat exchanger coupled with an ORC for geothermal energy. The ORC fluid is isobutane and the condenser is air-cooled using compact **fin-and-tube heat exchangers**, as is often the case (Hammons, 2007). A specific sizing of the heat exchanger is made in order to minimise the fans’ power consumption. The design of the dry cooling tower and the evaluation of fans power are detailed.

4.3.3.5 Heat exchanger modelling

Calise et al. (2014) developed a simulation model in order to investigate energetic and economic performance of an organic Rankine cycle powered by a medium temperature heat source. The heat exchanger modelling is based on **shell & tubes heat exchanger** geometry with single shell and double tube pass in E configuration. Shell and tube heat exchanger has been chosen because it shows great flexibility in terms of heat power transferred between hot and cold fluids, high operating pressure and temperature, high availability of construction materials, high value of both heat power transferred/weight and volume ratio, and finally low costs.

Imran et al. (2016) modelled a complete ORC system, the authors developed an independent model of each component: evaporator, condenser, expander and the working fluid pump. The condenser model has been constructed on the basis of a **plate-type heat exchanger** (chevron plate profile, see Figure 24 and Table 24).

Usman et al. (2017) built an ORC model based on plate-type heat exchangers. They investigate the selection of wet or dry cooling systems for low temperature ORC systems based on different climate conditions. The condenser modelling is based on a **plate-type condenser**. Table 28 indicates the specifications of the tested heat exchanger.

Table 28. Experimental validation details of heat exchanger condensing temperature prediction model.

Details of experimentally tested heat exchanger			
No. of plates	50	Plate space b	0.002 m
Chevron angle β	30°	No. of hot channels	24
Plate width W_e	0.244 m	No. of cold channels	25
VPCD	0.441 m	Working fluid	R245fa
		Sink fluid	Water

Sun et al. (2018) analysed the influence of the evaporator Pinch Point Temperature Difference (PPTD) on a geothermal ORC system economics with consideration of the drilling cost. The working fluid evaporating temperatures are optimised in this study for brine inlet temperatures from 100°C to 150°C and evaporator PPTDs from 4°C to 15°C. Isobutane is the working fluid. Heat transfer model is made assuming the preheater, evaporator, desuperheater and condenser are **counter-flow shell-and-tube exchangers**. **Carbon steel** with a carbon content of 0.5% was selected as the tube material with a tube thermal conductivity of 31 W/(m·K).

Walraven et al. (2014) implemented heat exchanger models in low-temperature binary cycle systems. Both **shell-and-tube heat exchangers** and **plate heat exchangers** are discussed. The influence of the heat-source-inlet temperature, heat-source-outlet temperature, total heat exchanger surface, cooling-fluid inlet temperature and the cooling fluid mass flow rate on the performance of the power plant have also been investigated. The comparison between ORCs with the two different types of heat exchangers has been performed in a wide range of parameters and for many fluids. The authors showed that **ORCs with all plate heat exchangers perform mostly better** than ORCs with all shell-and-tube heat exchangers. The disadvantage of plate heat exchangers with an equal number of passes at both sides of the exchanger is that the geometry of both sides of the heat exchanger are identical, which can lead to an inefficient heat exchanger when the two fluid streams require strongly different channel geometries. **The working fluid always flows on the shell side**, so models for the pressure drop and heat-transfer coefficient in single-phase flow, evaporation and condensation in a TEMA E shell have been used. The tube-side fluid (the heat source and the cooling fluid) is always single phase. The considered plate heat exchanger geometry is based on plates with chevron, also known as herringbone or corrugations (see Figure 27). The number of passes on both sides of the heat exchangers have been assumed to be equal.

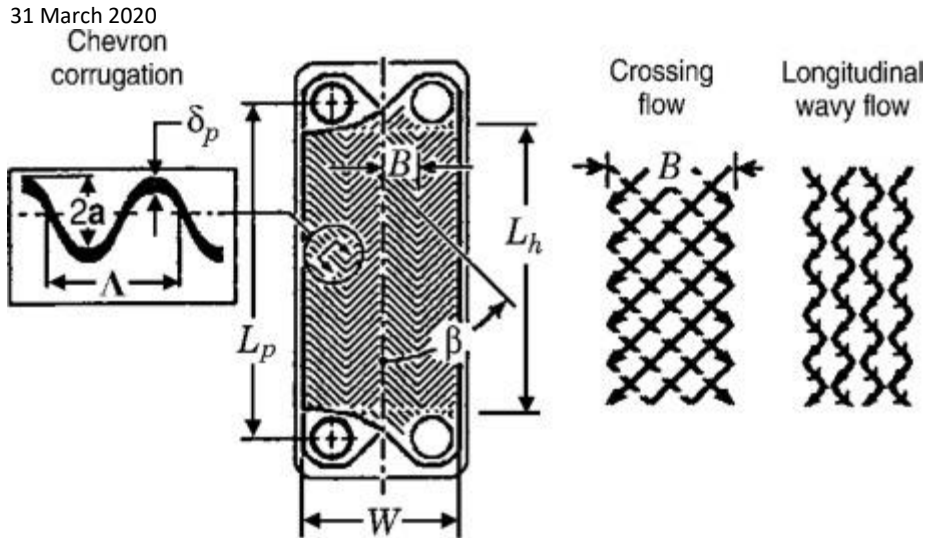


Figure 27: Geometrical parameters of a chevron plate (Walraven et al., 2014)

As a conclusion, in geothermal power plants, heat exchangers involved in the ORC, evaporators and condenser, can be **plate or tube-shell** depending on the scale of the geo-plant. For an installed generating capacity of **lower than tens of kilowatts, the plate heat exchanger** can be used. For an installed generating capacity of **higher than hundreds of kilowatts, the shell and tube heat exchanger** can be used (Li et al., 2015; Colonna et al., 2015).

According to Zarrouk and Moon (2014), the plate type heat exchanger is used for both low temperature and pressure in direct use applications, and shell and tube type for the high temperature and pressure associated with power generation and some of the higher temperature direct use. Geothermal shell and tube heat exchangers are all designed to have the geothermal (primary) fluid flowing inside the tubes, while the other (secondary) clean fluid flows on the shell side. This is to facilitate heat exchanger cleaning from the precipitation of solids and mineral deposition. This is also the main reason for not using a U-tube heat exchanger type which would be too difficult to clean.

4.3.3.6 Patents analysis

Among the corpus of 100 patents, 31 concern the heat exchanger technology. 26 of these refer to **shell-and-tube geometry** (tube bundle, tube fins,...). Only 5 patents deal with plate technology.

Ormat patents:

Ormat owns 100 patents concerning ORC in geothermal power plant. Examples of their geothermal power plants are illustrated in Figure 28:



Figure 28 Selected Ormat geothermal power plants

Figure 29 illustrates some patents for air-cooled condensers. Some of their patents concern fin configuration for air-cooled heat exchanger tubes as well as air-cooled condenser configuration.

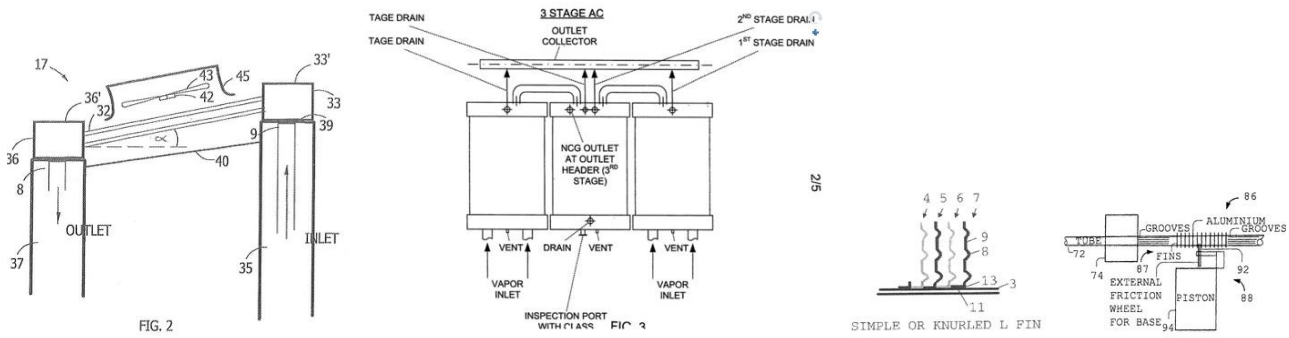


Figure 29 : Illustrations of some of the ORMAT patents (WO2019/130212, 2018; WO2014/140755, 2014 ; US9360258, 2013).

In the US patent (US5816048, 1995) entitled ‘Method for utilising acidic geothermal fluid for generating power in a rankine cycle power plant’, their claims state that the vaporiser preferably should be constructed from **titanium** or other corrosion resistant material, such as a **stainless steel**, coated **steel**, etc for maximum resistance to the corrosive effects of the steam (pH less than about 3.5) on the steam-side of the vaporiser.

The preheater likewise is preferably constructed of **titanium**, or other corrosion resistant material. Preferably, the preheater is a **plate-type heat exchanger** rather than a shell-and-tube type. However, if necessary and preferred, caustic soda or other suitable pH raising chemicals can be added to the geothermal fluid, brine and/or steam, or steam condensate.

Turboden:

Turboden propose patents based on Shell & Tube geometry as illustrated in Figure 30:

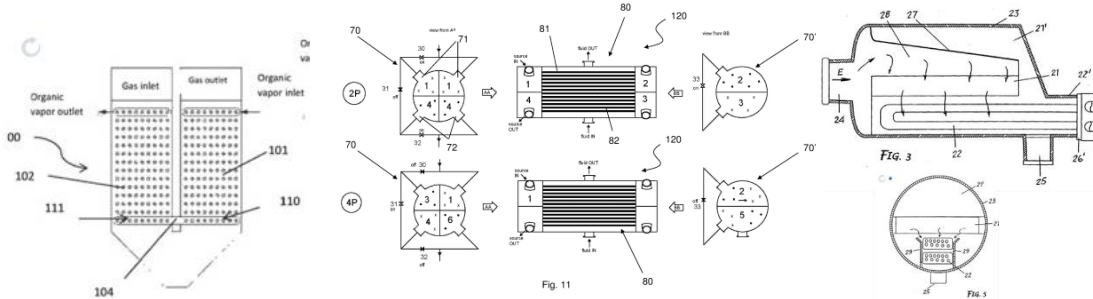


Figure 30 : Illustrations of TURBODEN patents based on tubes technology (EP3420204, 2016; EP3593077, 2017; EP1426565, 2002).

High quality, corrosion-resistant materials can be used for construction, such as **stainless steel** (for example with a % Cr greater than 16%), or **titanium or nickel alloys**.

Atlas Copco:

Patents illustrated in Figure 31 mainly concern shell & tube heat exchangers.

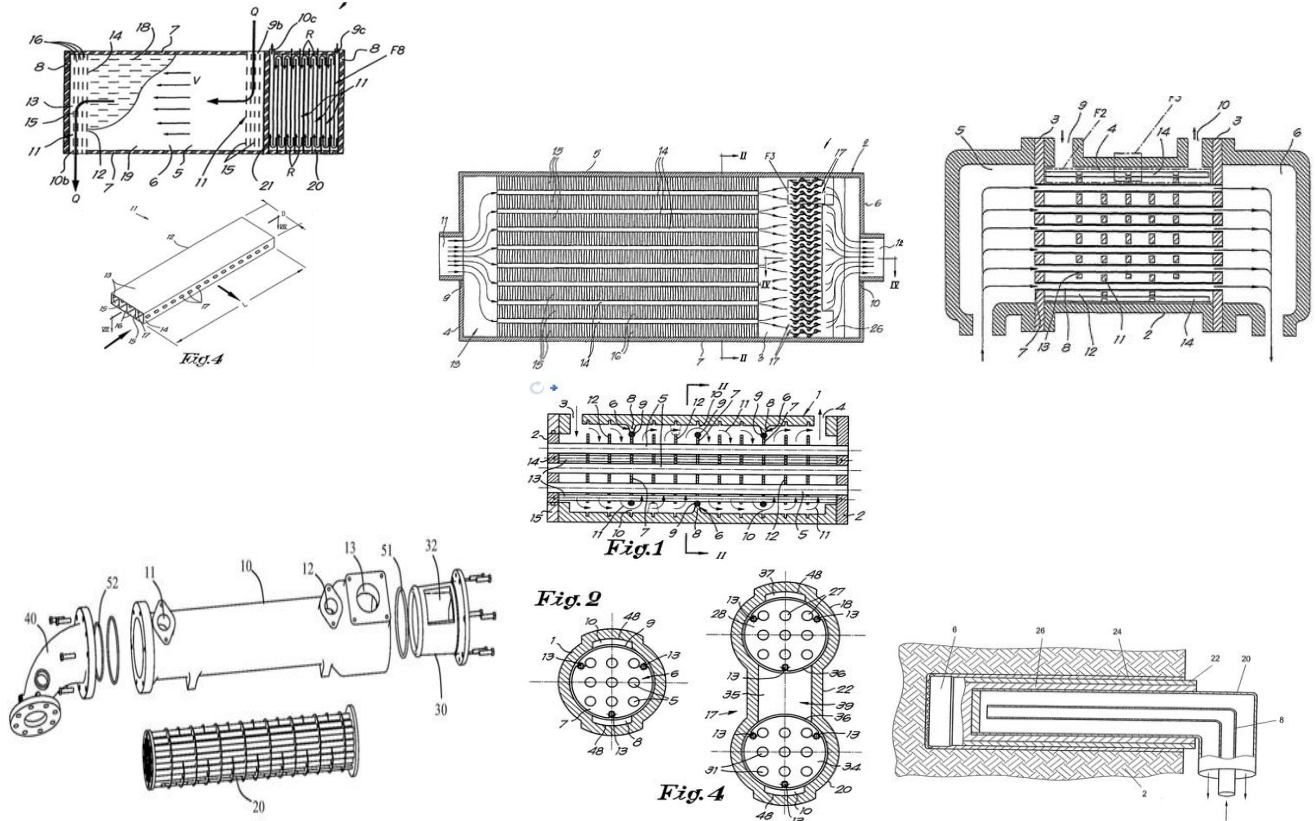


Figure 31 : Illustrations of ATLAS COPCO patents based on shell-and-tube technology (EP2417413, 2009; EP1711248, 2004; EP2480850, 2016; CN209212506, 2018; EP0628779, 1993; WO2007/070905, 2006).

Kaori :

Kaori proposes technologies based on brazed plate heat exchangers (Figure 32). Their technology is used where frequent thermal or pressure shocks are expected in the refrigerant evaporator.

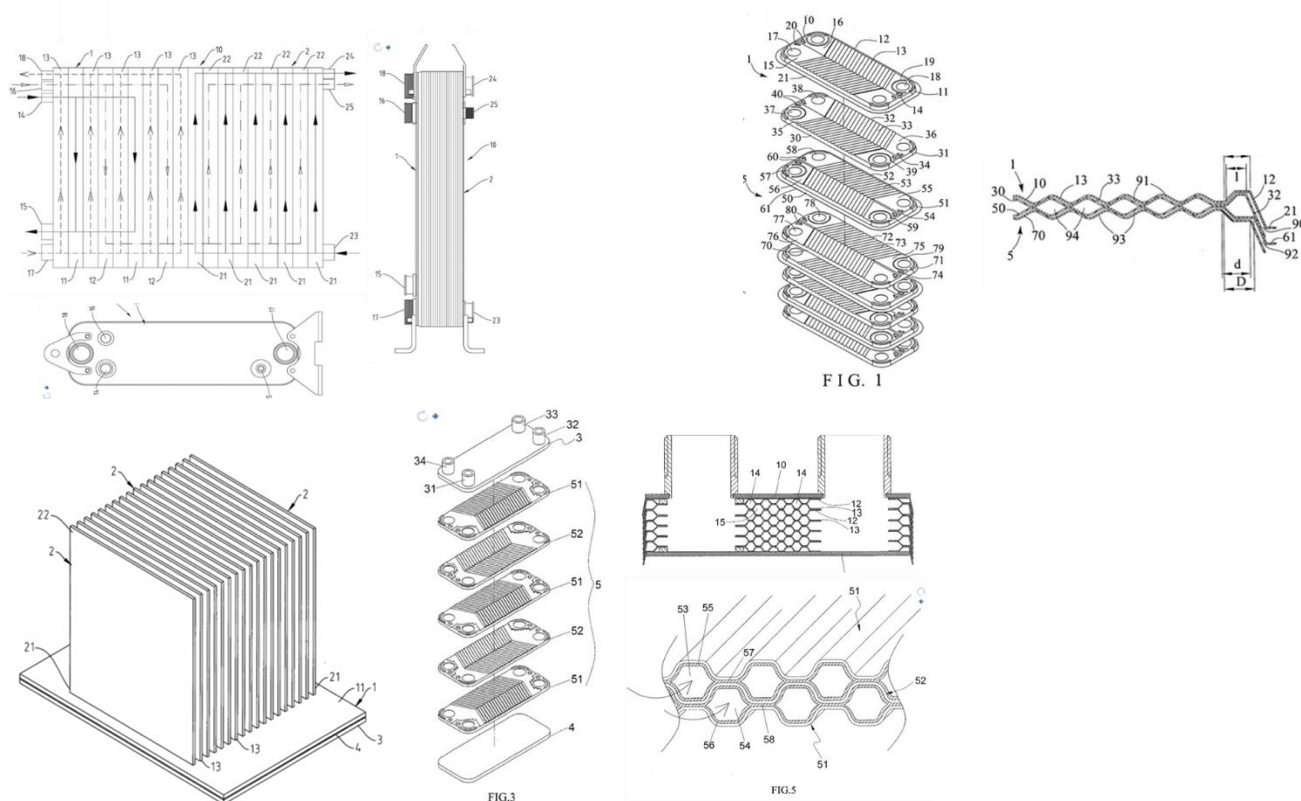


Figure 32 : Illustrations of KAORI patents based on brazed plate-type heat exchangers (CN209558724, 2018; US20160040943, 2006; TWM507159, 2015; DE202011100416, 2011).

The base plate may be made of **stainless steel**. The inner wall of the first channel has a first **protective layer** and the inner wall of the second flow channel has a second protective layer. The protective layers can be formed from a **copper-nickel alloy**.

5. CONCLUSIONS

- Major types of geothermal power plants are: dry steam, single-flash, double-flash and **binary-cycle plants**.
- Regarding **working fluids**:
 - Main working fluids at commercial scale are n-pentane, isopentane, R134a and R245fa.
 - Binary power units running on hydrocarbons are equal to approximately 83% of the total installed capacity of all the binary power units in the world.
 - Relatively cheap hydrocarbons (pentane, isobutane, isopentane, etc) characterised by good thermodynamic and thermal properties are explosive and flammable and can be used in open type power plants, which is not always acceptable to the areas with negative winter temperatures.
 - For low and mid-range heat source temperatures (<150-200°C), the hydrofluorocarbons (HFC) **R134a** and **R245fa** seem preferred.
 - Simulations and thermo-economic calculations show that at low geofluid temperatures (< 200°C), using refrigerants (such as HFC) as the ORC working fluid results in slightly higher performance than hydrocarbons.
- Regarding **heat exchanger technologies**:
 - For an installed generating capacity of **higher than hundreds of kilowatts**, as well as for high temperature and pressure, **shell and tube heat exchangers** are preferred.

Date: 31 March 2020

- The power consumption of the cooling system of the ORC may reach up to **30% of the turbine output**.
- **Evaporators** are mostly **shell-and-tube heat exchangers**. Working fluid is on the shell side while geothermal brine is on the tube side.
- **Recuperators** and **pre-heaters** are **plate-type heat exchangers**.
- Regarding evaporators and condensers, plate heat exchangers are interesting to reduce heat exchanger surfaces but they are mainly considered for **calculations**.
- **Water-cooled condensers** are mostly **shell-and-tube heat exchangers** with water inside the tubes and the working fluid on the shell side.
- **Few plate-type condensers** exist with welded or brazed stainless steel plates (eg. Husavik, Iceland and Kaori patents).
- **Fin-and-tube heat exchangers** are used as air-cooled condensers.
- **Air-cooled condensers are more expensive** (surface area of a water-cooled condenser can be approximately 25 to 40times less than an air-cooled one) but **mainly used** to limit water consumption or in extreme climatic conditions.
- S&T heat exchangers are made of **stainless steel (tubes)** to handle corrosion and scaling while the shell is made of **carbon steel**.
- Plate material will be stainless steel (around 10% of the total HX weight, therefore there is no interest in replacing the stainless steel with carbon steel). The housing is made of carbon steel with a stainless steel liner.

As a conclusion, the most relevant heat exchangers for large-scale geothermal power plants are **shell-and-tube heat exchangers**. However plate-type heat exchangers are most cost-effective (lower heat transfer surface). The proposed configurations for GeoHex tests are:

- For evaporator:
 - Carbon steel shell-and-tube heat exchanger.
 - Stainless steel plate-type heat exchanger. According to the operating pressure (to be defined and confirmed), welded or brazed plates will be used on the working fluid side. This would mean that no material deposit could be made on the evaporation side in the plate-type heat exchanger.
- For condensers:
 - Carbon steel shell-and-tube heat exchanger (water-cooled condenser).
 - Fin-and-tube heat exchanger (air-cooled condenser, material to be defined).
- For liquid/liquid heat exchanger:
 - Carbon steel shell-and-tube heat exchanger.
 - Stainless steel plate-type heat exchanger.

6. REFERENCES

Abisa, M.T., 2002. Geothermal binary plant operation and maintenance systems with Svartsengi power plant as a case study. Geothermal Training in Iceland: Reports of the United Nations University Geothermal Training Programme in geothermal exploration.

Alimonti, C., Conti, P., Soldo, E., 2019. A comprehensive exergy evaluation of a deep borehole heat exchanger coupled with a ORC plant: the case study of Campi Flegrei. Energy 189, 116100. <https://doi.org/10.1016/j.energy.2019.116100>

Altun, A.F., Kilic, M., 2020. Thermodynamic performance evaluation of a geothermal ORC power plant. Renewable Energy 148, 261–274. <https://doi.org/10.1016/j.renene.2019.12.034>

Arslan, O., Kose, R., 2010. Exergoeconomic optimization of integrated geothermal system in Simav, Kutahya. Energy Conversion and Management 51, 663–676. <https://doi.org/10.1016/j.enconman.2009.11.010>

Astolfi, M., Romano, M.C., Bombarda, P., Macchi, E., 2014. Binary ORC (organic Rankine cycles) power plants for the exploitation of medium–low temperature geothermal sources – Part A: Thermodynamic optimization. Energy 66, 423–434. <https://doi.org/10.1016/j.energy.2013.11.056>

Brasz JJ, Biederman BP, Holdmann G. 2005, Power Production from a Moderate Temperature – Geothermal Resource GRC Annual Meeting, Reno, NV, USA.

Budisulistyo, D., Krumdieck, S., 2015. Thermodynamic and economic analysis for the pre-feasibility study of a binary geothermal power plant. Energy Conversion and Management 103, 639–649. <https://doi.org/10.1016/j.enconman.2015.06.069>

Calise, F., Capuozzo, C., Carotenuto, A., Vanoli, L., 2014. Thermoeconomic analysis and off-design performance of an organic Rankine cycle powered by medium-temperature heat sources. Solar Energy 103, 595–609. <https://doi.org/10.1016/j.solener.2013.09.031>

Chen, F., Liu, L., Peng, J., Ge, Y., Wu, H., Liu, W., 2019. Theoretical and experimental research on the thermal performance of ocean thermal energy conversion system using the rankine cycle mode. Energy 183, 497–503. <https://doi.org/10.1016/j.energy.2019.04.008>

Chen, H., Goswami, D.Y., Stefanakos, E.K., 2010. A review of thermodynamic cycles and working fluids for the conversion of low-grade heat. Renewable and Sustainable Energy Reviews 14, 3059–3067. <https://doi.org/10.1016/j.rser.2010.07.006>

Colonna, P., Casati, E., Trapp, C., Mathijssen, T., Larjola, J., Turunen-Saaresti, T., Uusitalo, A., 2015. Organic Rankine Cycle Power Systems: From the Concept to Current Technology, Applications, and an Outlook to the Future. Journal of Engineering for Gas Turbines and Power 137. <https://doi.org/10.1115/1.4029884>

DiPippo, R., 2004. Second Law assessment of binary plants generating power from low-temperature geothermal fluids. Geothermics 33, 565–586. <https://doi.org/10.1016/j.geothermics.2003.10.003>

DiPippo, R., 2016. Geothermal power plants: principles, applications, case studies and environmental impact, Fourth edition. ed. Butterworth-Heinemann is an imprint of Elsevier, Amsterdam ; Boston.

Erdogan, A., Colpan, C.O., Cakici, D.M., 2017. Thermal design and analysis of a shell and tube heat exchanger integrating a geothermal based organic Rankine cycle and parabolic trough solar collectors. Renewable Energy 109, 372–391. <https://doi.org/10.1016/j.renene.2017.03.037>

Eyerer, S., Schiffelechner, C., Hofbauer, S., Bauer, W., Wieland, C., Spliethoff, H., 2020. Combined heat and power from hydrothermal geothermal resources in Germany: An assessment of the potential. Renewable and Sustainable Energy Reviews 120, 109661. <https://doi.org/10.1016/j.rser.2019.109661>

Franco, A., 2011. Power production from a moderate temperature geothermal resource with regenerative Organic Rankine Cycles. *Energy for Sustainable Development* 15, 411–419. <https://doi.org/10.1016/j.esd.2011.06.002>

Ganjehsarabi, H., Gungor, A., Dincer, I., 2012. Exergetic performance analysis of Dora II geothermal power plant in Turkey. *Energy* 46, 101–108. <https://doi.org/10.1016/j.energy.2012.02.039>

Guzović, Z., Majcen, B., Cvetković, S., 2012. Possibilities of electricity generation in the Republic of Croatia from medium-temperature geothermal sources. *Applied Energy* 98, 404–414. <https://doi.org/10.1016/j.apenergy.2012.03.064>

Hærvig, J., Sørensen, K., Condra, T.J., 2016. Guidelines for optimal selection of working fluid for an organic Rankine cycle in relation to waste heat recovery. *Energy* 96, 592–602. <https://doi.org/10.1016/j.energy.2015.12.098>

Hammons, T.J., 2007. Geothermal power generation: global perspectives; USA and Iceland; technology, direct uses, plants, and drilling. *International journal of power & energy systems* 27, 157.

Hettiarachchi, M., Golubovic, M., Worek, W., Ikegami, Y., 2007. Optimum design criteria for an Organic Rankine Cycle using low-temperature geothermal heat sources. *Energy* 32, 1698–1706. <https://doi.org/10.1016/j.energy.2007.01.005>

Hung, T.C., Wang, S.K., Kuo, C.H., Pei, B.S., Tsai, K.F., 2010. A study of organic working fluids on system efficiency of an ORC using low-grade energy sources. *Energy* 35, 1403–1411. <https://doi.org/10.1016/j.energy.2009.11.025>

Imran, M., Usman, M., Park, B.-S., Yang, Y., 2016. Comparative assessment of Organic Rankine Cycle integration for low temperature geothermal heat source applications. *Energy* 102, 473–490. <https://doi.org/10.1016/j.energy.2016.02.119>

Kahraman, M., Olcay, A.B., Sorgüven, E., 2019. Thermodynamic and thermoeconomic analysis of a 21 MW binary type air-cooled geothermal power plant and determination of the effect of ambient temperature variation on the plant performance. *Energy Conversion and Management* 192, 308–320. <https://doi.org/10.1016/j.enconman.2019.04.036>

Kanoglu, M., 2002. Exergy analysis of a dual-level binary geothermal power plant. *Geothermics* 31, 709–724. [https://doi.org/10.1016/S0375-6505\(02\)00032-9](https://doi.org/10.1016/S0375-6505(02)00032-9)

Kanoglu, M., Bolatturk, A., 2008. Performance and parametric investigation of a binary geothermal power plant by exergy. *Renewable Energy* 33, 2366–2374. <https://doi.org/10.1016/j.renene.2008.01.017>

Keçebaş, A., Gökgedik, H., 2015. Thermodynamic evaluation of a geothermal power plant for advanced exergy analysis. *Energy* 88, 746–755. <https://doi.org/10.1016/j.energy.2015.05.094>

Kose, R., 2007. Geothermal energy potential for power generation in Turkey: A case study in Simav, Kutahya. *Renewable and Sustainable Energy Reviews* 11, 497–511. <https://doi.org/10.1016/j.rser.2005.03.005>

Li, T., Wang, Q., Zhu, J., Hu, K., Fu, W., 2015. Thermodynamic optimization of organic Rankine cycle using two-stage evaporation. *Renewable Energy* 75, 654–664. <https://doi.org/10.1016/j.renene.2014.10.058>

Mahmoudi, A., Fazli, M., Morad, M.R., 2018. A recent review of waste heat recovery by Organic Rankine Cycle. *Applied Thermal Engineering* 143, 660–675. <https://doi.org/10.1016/j.applthermaleng.2018.07.136>

Mendrinós, D., Kontoleontos, E., Karytsas, C., 2006. Geothermal binary plants: water or air cooled, in: *Proceedings of the Engine Workshop 5 on Electricity Generation from Enhanced Geothermal Systems*. Strasbourg, France, pp. 1–10.

Date: 31 March 2020

Mlcak, H., Miroli, M., Hjartarson, H., Húsavík, O., Ralph, M., 2002. Notes from the North: A report on the debut year of the 2 MW Kalina Cycle® geothermal power plant in Húsavík, Iceland. *Transactions-Geothermal Resources Council* 715–718.

Moya, P., DiPippo, R., 2007. Unit 5 bottoming binary plant at Miravalles geothermal field, Costa Rica: Planning, design, performance and impact. *Geothermics* 36, 63–96. <https://doi.org/10.1016/j.geothermics.2006.10.003>

Muhammad, U., Imran, M., Lee, D.H., Park, B.S., 2015. Design and experimental investigation of a 1kW organic Rankine cycle system using R245fa as working fluid for low-grade waste heat recovery from steam. *Energy Conversion and Management* 103, 1089–1100. <https://doi.org/10.1016/j.enconman.2015.07.045>

Nakaoka, T., Uehara, H., 1988a. Performance test of a shell-and-plate type evaporator for OTEC. *Experimental Thermal and Fluid Science* 1, 283–291. [https://doi.org/10.1016/0894-1777\(88\)90008-8](https://doi.org/10.1016/0894-1777(88)90008-8)

Nakaoka, T., Uehara, H., 1988b. Performance test of a shell-and-plate-type condenser for OTEC. *Experimental Thermal and Fluid Science* 1, 275–281. [https://doi.org/10.1016/0894-1777\(88\)90007-6](https://doi.org/10.1016/0894-1777(88)90007-6)

Pambudi, N.A., 2018. Geothermal power generation in Indonesia, a country within the ring of fire: Current status, future development and policy. *Renewable and Sustainable Energy Reviews* 81, 2893–2901. <https://doi.org/10.1016/j.rser.2017.06.096>

Pasek, A.D., Fauzi Soelaiman, T.A., Gunawan, C., 2011. Thermodynamics study of flash–binary cycle in geothermal power plant. *Renewable and Sustainable Energy Reviews* 15, 5218–5223. <https://doi.org/10.1016/j.rser.2011.05.019>

Putera, A.D.P., Hidayah, A.N., Subiantoro, A., 2019. Thermo-Economic Analysis of A Geothermal Binary Power Plant in Indonesia—A Pre-Feasibility Case Study of the Wayang Windu Site. *Energies* 12, 4269. <https://doi.org/10.3390/en12224269>

Saleh, B., Koglbauer, G., Wendland, M., Fischer, J., 2007. Working fluids for low-temperature organic Rankine cycles. *Energy* 32, 1210–1221. <https://doi.org/10.1016/j.energy.2006.07.001>

Schochet, D.N., 1997. Performance of ORMAT geothermal binary and combined steam/binary cycle power plants with moderate and high temperature resources. *Renewable Energy* 10, 379–387.

Sun, J., Liu, Q., Duan, Y., 2018. Effects of evaporator pinch point temperature difference on thermo-economic performance of geothermal organic Rankine cycle systems. *Geothermics* 75, 249–258. <https://doi.org/10.1016/j.geothermics.2018.06.001>

Tchanche, B.F., Lambrinos, G., Frangoudakis, A., Papadakis, G., 2011. Low-grade heat conversion into power using organic Rankine cycles – A review of various applications. *Renewable and Sustainable Energy Reviews* 15, 3963–3979. <https://doi.org/10.1016/j.rser.2011.07.024>

Tomarov, G.V., Nikol'skii, A.I., Semenov, V.N., Shipkov, A.A., 2010. Construction of Russia's pilot binary power unit at the pauzhet geothermal power station. *Thermal Engineering* 57, 925–930. <https://doi.org/10.1134/S0040601510110030>

Tomarov, G.V., Nikol'skii, A.I., Semenov, V.N., Shipkov, A.A., 2014. Equipment of the binary-cycle geothermal power unit at the Pauzhet geothermal power station. *Thermal Engineering* 61, 406–410. <https://doi.org/10.1134/S0040601514060093>

Tomarov, G.V., Shipkov, A.A., 2017. Modern geothermal power: Binary cycle geothermal power plants. *Thermal Engineering* 64, 243–250. <https://doi.org/10.1134/S0040601517040097>

Unverdi, M., Cerci, Y., 2013. Performance analysis of Germencik Geothermal Power Plant. *Energy* 52, 192–200. <https://doi.org/10.1016/j.energy.2012.12.052>

- Usman, M., Imran, M., Yang, Y., Lee, D.H., Park, B.-S., 2017. Thermo-economic comparison of air-cooled and cooling tower based Organic Rankine Cycle (ORC) with R245fa and R1233zde as candidate working fluids for different geographical climate conditions. *Energy* 123, 353–366. <https://doi.org/10.1016/j.energy.2017.01.134>
- Vivian, J., Manente, G., Lazzaretto, A., 2015. A general framework to select working fluid and configuration of ORCs for low-to-medium temperature heat sources. *Applied Energy* 156, 727–746. <https://doi.org/10.1016/j.apenergy.2015.07.005>
- Walraven, D., Laenen, B., D’haeseleer, W., 2014. Comparison of shell-and-tube with plate heat exchangers for the use in low-temperature organic Rankine cycles. *Energy Conversion and Management* 87, 227–237. <https://doi.org/10.1016/j.enconman.2014.07.019>
- Welzl, M., Heberle, F., Brüggemann, D., 2020. Experimental evaluation of nucleate pool boiling heat transfer correlations for R245fa and R1233zd(E) in ORC applications. *Renewable Energy* 147, 2855–2864. <https://doi.org/10.1016/j.renene.2018.09.093>
- Yildirim, D., Ozgener, L., 2012. Thermodynamics and exergoeconomic analysis of geothermal power plants. *Renewable and Sustainable Energy Reviews* 16, 6438–6454. <https://doi.org/10.1016/j.rser.2012.07.024>
- Zare, V., 2015. A comparative exergoeconomic analysis of different ORC configurations for binary geothermal power plants. *Energy Conversion and Management* 105, 127–138. <https://doi.org/10.1016/j.enconman.2015.07.073>
- Zarrouk, S.J., Moon, H., 2014. Efficiency of geothermal power plants: A worldwide review. *Geothermics* 51, 142–153. <https://doi.org/10.1016/j.geothermics.2013.11.001>
- Zarrouk, S.J., Woodhurst, B.C., Morris, C., 2014. Silica scaling in geothermal heat exchangers and its impact on pressure drop and performance: Wairakei binary plant, New Zealand. *Geothermics* 51, 445–459. <https://doi.org/10.1016/j.geothermics.2014.03.005>
- Zeyghami, M., 2015. Performance analysis and binary working fluid selection of combined flash-binary geothermal cycle. *Energy* 88, 765–774. <https://doi.org/10.1016/j.energy.2015.05.092>